Title

Characterization of defense responses against bacterial pathogens in duckweeds lacking EDS1

Journal

New Phytologist, 236(5)

ISSN

0028-646X

Authors

Baggs, Erin L
Tiersma, Meije B
Abramson, Brad W
et al.

Publication Date

2022-12-01

DOI

10.1111/nph.18453

Peer reviewed

New Phytologist

Characterization of defense responses against bacterial pathogens in duckweeds lacking EDS1

Erin L. Baggs[1], Meije B. Tiersma[1], Brad W. Abramson[2], Todd P. Michael[2] and Ksenia V. Krasileva[1]

[1]Department of Plant and Microbial Biology, University of California Berkeley, Berkeley, CA 94720, USA; [2]Plant Molecular and Cellular Biology Laboratory, The Salk Institute for Biological Studies, La Jolla, CA 92037, USA

Author for correspondence:
Ksenia V. Krasileva
Email: kseniak@berkeley.edu

Received: *20 April 2022*
Accepted: *19 August 2022*

New Phytologist (2022) **236:** 1838–1855
doi: 10.1111/nph.18453

Key words: antimicrobial proteins, duckweed, EDS1, plant immunity, *Pseudomonas syringae*, transcriptional response.

Summary

• *ENHANCED DISEASE SUSCEPTIBILITY 1 (EDS1)* mediates the induction of defense responses against pathogens in most angiosperms. However, it has recently been shown that a few species have lost *EDS1*. It is unknown how defense against disease unfolds and evolves in the absence of *EDS1*. We utilize duckweeds; a collection of aquatic species that lack *EDS1*, to investigate this question.

• We established duckweed-*Pseudomonas* pathosystems and used growth curves and microscopy to characterize pathogen-induced responses. Through comparative genomics and transcriptomics, we show that the copy number of infection-associated genes and the infection-induced transcriptional responses of duckweeds differ from other model species.

• Pathogen defense in duckweeds has evolved along different trajectories than in other plants, including genomic and transcriptional reprogramming. Specifically, the miAMP1 domain-containing proteins, which are absent in Arabidopsis, showed pathogen responsive upregulation in duckweeds. Despite such divergence between Arabidopsis and duckweed species, we found conservation of upregulation of certain genes and the role of hormones in response to disease.

• Our work highlights the importance of expanding the pool of model species to study defense responses that have evolved in the plant kingdom independent of *EDS1*.

Introduction

Receptors and signaling components of the plant immune signal network likely evolved before the divergence of flowering plants 181 million years ago (Ma; Kumar *et al.*, 2017). The two primary layers of plant innate immunity, microbe-associated molecular pattern (MAMP)-triggered immunity (MTI) and effector-triggered Immunity (ETI; Alhoraibi *et al.*, 2019), form an intricate network of cross-amplifying pathways (Ngou *et al.*, 2021; Tian *et al.*, 2021; Yuan *et al.*, 2021a). The shared evolutionary history of MTI and ETI suggests that they intricately co-evolved and are foundational for immunity in flowering plants. ENHANCED DISEASE SUSCEPTIBILITY 1 (EDS1) is a central hub in MTI and ETI signal transduction and amplification. Mutations abolishing activity of EDS1 compromise ETI and MTI (Wagner *et al.*, 2013; Cui *et al.*, 2017; Pruitt *et al.*, 2021). Surprisingly, genomic studies have revealed several angiosperms that thrive in their natural environments without EDS1, including the Lemnaceae (Baggs *et al.*, 2020). It is unknown how the response to bacterial pathogens would proceed or evolve in the absence of a functional EDS1.

Lemnaceae diverged from other monocots at 128 Ma (Kumar *et al.*, 2017). The common ancestor of the Lemnaceae was present in a freshwater aquatic environment and had a reduced body plan of a frond (a fused stem and leaf) and root (Acosta *et al.*, 2021). Genera within the Lemnaceae include *Spirodela*, *Landoltia*, *Lemna*, *Wolffia* and *Wolffiella*, all of which primarily reproduce through asexual budding (Bog *et al.*, 2019). The small genome and body plan is conducive to the Lemnaceae's rapid lifecycle with a doubling time of as little as 34 h (Michael *et al.*, 2020). Lemnaceae are very easy to grow in the laboratory which has stimulated research into their use as biofuels (Su *et al.*, 2014; Van Hoeck *et al.*, 2015; Xu *et al.*, 2018) and enabled the growth of genomic resources (Wang *et al.*, 2014; Michael *et al.*, 2017, 2020; Hoang *et al.*, 2020; Abramson *et al.*, 2021). *Spirodela polyrhiza* has a small genome of 158 Mb and has lost members of the expansin and cellulose biosynthesis families (Wang *et al.*, 2014; Michael *et al.*, 2017). *Wolffia australiana* has lost light signaling pathways and root development pathways, which is not surprising given the absence of roots in *Wolffia* (Michael *et al.*, 2020). In addition to developmental pathways lost in other Lemnaceae, *S. polyrhiza* was previously shown to have lost *EDS1* (Baggs *et al.*, 2020), however the extent of immune pathway loss in other Lemnaceae remained unclear.

Given the absence of the EDS1 pathway in *S. polyrhiza* (Baggs *et al.*, 2020), we hypothesized that duckweeds could be a model system for understanding EDS1-independent innate immunity. Lemnaceae are globally distributed and only absent from the

Arctic and Antarctica (Landolt, 1992; Crawford *et al.*, 2006); several Lemnaceae species are invasive species (Abramson *et al.*, 2021; CABI, 2021). The wide distribution of duckweeds means their range overlaps with several model plant pathogens: *Pseudomonas syringae* pv *tomato* DC3000, *P. syringae* pv *syringae*, *Xanthomonas perforans*, *Xanthomonas euvesicatoria* (Cai *et al.*, 2011; Potnis *et al.*, 2015; Gutiérrez-Barranquero *et al.*, 2019), and many others for which genomic and genetic resources are available. These pathogens often have devastating effects on crop plants yield and value (Martins *et al.*, 2018).

Microbe-associated molecular pattern-triggered immunity immune signaling is triggered by the recognition of conserved molecular patterns through pattern recognition receptors (PRRs) and their respective co-receptors. There are two main types of PRRs: receptor-like kinases (RLKs) and receptor-like proteins (RLPs), that lack an intracellular kinase domain (Lolle *et al.*, 2020; Offor *et al.*, 2020; Yuan *et al.*, 2021b). Substantial differences exist between RLP and RLK signaling pathways: immune signaling through the RLP and Suppressor of BIR1 (SOBIR1) co-receptor pathway genetically requires *EDS1*, *Phytoalexin Deficient 4* (*PAD4*) and *Resistance to Powdery Mildew 8 Nucleotide-binding Leucine-rich repeat Receptors* (*RNLs*) and results in higher levels of ethylene and phytoalexins production, as well as Pathogenesis Related 1 gene expression (Pruitt *et al.*, 2021; Tian *et al.*, 2021). *Pathogenesis Related* (*PR*) genes are characterized by their rapid upregulation after pathogen infection, they include several antimicrobial genes with different modes of action (glucanase, thaumatin, chitinase, thionin and defensin; Ali *et al.*, 2018). There are many antimicrobial peptides that are not classed as *PR* genes, such as proteins with the MiAMP1 domain (Marcus *et al.*, 1997; McManus *et al.*, 1999; Stephens *et al.*, 2005). The MiAMP1 domain was identified as a key structural motif in the MiAMP1 protein named after its isolation from *Macadamia integrifolia* and its antimicrobial activity (Marcus *et al.*, 1997; Stephens *et al.*, 2005). Furthermore, transgenic canola expressing MiAMP1 showed enhanced resistance to the pathogen *Leptosphaeria maculans* (Kazan *et al.*, 2002). The diversity and modes of action of these antimicrobials remains poorly understood.

Receptor-like protein and RLK activation primes the cell to initiate a stronger immune response upon Nucleotide-binding Leucine-rich repeat Receptors (NLRs) perception of intracellular changes caused by pathogen-derived effectors (Tian *et al.*, 2021). Conserved domain architecture and signaling specificities of NB-ARC domain-containing proteins allow their classification into RNLs, coiled-coil NLRs (CNLs), Toll/interleukin-1 receptor NLRs (TNLs) and TIR-NBARC-Tetratricopeptide repeats (TNP; Nandety *et al.*, 2013; Shao *et al.*, 2016, 2019; Baggs *et al.*, 2017; Johanndrees *et al.*, 2021). Disease resistance mediated by TNLs and some CNLs is genetically dependent on RNLs and the lipase-like proteins EDS1 and PAD4 or SAG101. The recognition of pathogen presence by an NLR typically leads to qualitative resistance where the plant shows a discrete resistant phenotype.

In the absence of NLR triggered ETI, plants are not necessarily susceptible to a pathogen. Instead, quantitative resistance may be observed where extent of resistance is more variable and, in some cases, underpinned by hundreds of loci (Corwin & Kliebenstein, 2017). Mechanisms implicated in quantitative resistance include defensins, pathogenesis-related proteins, secondary metabolite enzymes and pathogen-induced phytohormones accumulation (Corwin & Kliebenstein, 2017). Qualitative disease resistance follows mendelian patterns of inheritance of resistance of individuals to a given pathogen genotype. Typically, the mechanism of qualitative resistance involves MTI and ETI. In contrast, the level of quantitative resistance spans a continuous distribution and is typically governed by several small effect loci.

In this study, we investigated the phenotypic, genomic, and transcriptomic characteristics of duckweeds in response to *Pseudomonas* phytopathogens. We found a stepwise reduction of conserved ETI pathways within the Lemnaceae and loss of MTI immune pathway components in *W. australiana*. However, we observed a shared expansion of the MiAMP1 protein family across Lemnaceae. Additionally, we noticed species-specific responses to pathogen treatments among duckweed species. We investigated the transcriptional response to pathogens of duckweed species, a system which is adapted to the absence of EDS1-mediated immune signaling cascades. Our study highlights duckweeds as a rapid growth, high throughput, minimalist MTI-ETI model organism. As such, it could be utilized to expedite our understanding of EDS1-independent MTI-ETI mechanisms of immunity as well as to dissect mechanisms of quantitative resistance.

Materials and Methods

Landoltia punctata clone 5635 DNA isolation and sequencing

Landoltia punctata clone 5635 (Lp5635, formerly DWC138) was received from the Rutgers Duckweed Stock Collective (RDSC; http://www.ruduckweed.org/). Lp5635 was collected, patted dry to remove excess water and flash frozen in liquid nitrogen. Frozen tissue was ground with a mortar and pestle in liquid nitrogen. High molecular weight (HMW) DNA was isolated using a modified Bomb protocol (Oberacker *et al.*, 2019). DNA quality was assessed on a Bioanalyzer and HMW status was confirmed on an agarose gel. Libraries were prepared from HMW DNA using NEBnext (NEB, Beverly, MA, USA) and 2 × 150 bp paired end reads were generated on the Illumina NovaSeq (San Diego, CA, USA). Resulting raw sequence was only trimmed for adaptors, resulting >60× coverage of the diploid *L. punctata* genome (350 Mb).

Landoltia punctata clone 5635 genome assembly, gene prediction and annotation

Illumina paired end reads were assembled with SPADES (v.3.14.0) with the default settings (Bankevich *et al.*, 2012). Resulting contigs were annotated using a pipeline consisting of four major steps: repeat masking, transcript assembly, gene model prediction, and functional annotation as described (Abramson

et al., 2021). Repeats were identified using EDTA (v.1.9.8; Ou *et al.*, 2019) and these repeats were used for softmasking. RNA-sequencing (RNA-Seq) reads were aligned to the genomes using MINIMAP2 and assembled into transcript models using STRINGTIE (v.1.3.6). The soft-masked genome and STRINGTIE models were then processed by FUNANNOTATE (v.1.6; https://github.com/nextgenusfs/funannotate) to produce gene models. Predicted proteins were then functionally annotated using EGGNOG-MAPPER (v.2; Huerta-Cepas *et al.*, 2017).

Pathway ortholog identification

The genomes and proteomes used included *Arabidopsis thaliana* TAIR 10 (Lamesch *et al.*, 2012), *Solanum lycopersicum* ITAG2.3 (Tomato Genome Consortium, 2012), *Oryza sativa* v.7 (Ouyang *et al.*, 2007), *S. polyrhiza* v.2 (Wang *et al.*, 2014), *W. australiana* 8730 (Michael *et al.*, 2020), *Colocasia esculenta* (L.) Schott (*C. esculenta* S; Yin *et al.*, 2021) and *C. esculenta* Niue (*C. esculenta* N) (Atibalentja *et al.*, 2019). Proteome completeness was evaluated using BUSCO v.5 (Simão *et al.*, 2015; Table S1).

To date the loss of *EDS1*, *PAD4*, *ADR1* and *NDR1*, we ran a BLASTP search using the *O. sativa* and *A. thaliana* EDS1, PAD4, ADR1 and NDR1 proteins as queries against two Taro proteomes; *C. esculenta* (L.) Schott (*C. esculenta* S; Yin *et al.*, 2021) and *C. esculenta* N. If no ortholog was identified, we used TBLASTN to check this was not an artifact of annotation. To confirm orthologs, the Taro subject sequence was the query for BLASTP to the *O. sativa* and *A. thaliana* proteomes. Upon confirming the presence of *EDS1*, *PAD4*, *ADR1* and *NDR1* in Taro, we utilized TimeTree.org to estimate the time during which *EDS1*, *PAD4*, *ADR1* and *NDR1* were lost.

To identify orthologous genes, ORTHOFINDER (v.2.5.4; Emms & Kelly, 2019) was ran on *S. polyrhiza* 7498 (Wang *et al.*, 2014), *L. punctata* 5635, *W. australiana* 8730 (Michael *et al.*, 2020) and *A. thaliana* TAIR 10 (Lamesch *et al.*, 2012). Infection responsive *A. thaliana* genes were identified by literature searches (Table S2). The Arabidopsis GIDs were used to extract orthogroups containing Lemnaceae homologs which were cross checked using PHYTOZOME. Gene absence was verified using TBLASTN (Camacho *et al.*, 2009). For large gene family analysis of MiAMP1, RLK, RLP and NLRs, PFAMSCAN (Sarris *et al.*, 2016; Madeira *et al.*, 2019) was used to identify proteins with domains of interest (*e*-value = 10; MiAMP1, RLK, RLP and NB-ARC domains; Table S1). Receptor-like kinase, RLP and MiAMP1 protein sequences were aligned with MUSCLE v.3.8.1551 (Madeira *et al.*, 2019) and NB-ARC domains were aligned with hmmalign from HMMER3 (Wheeler & Eddy, 2013) to NB-ARC1-ARC2 (Bailey *et al.*, 2018). Alignments were manually curated using BELVU (Barson & Griffiths, 2016) and JALVIEW (Waterhouse *et al.*, 2009). Maximum likelihood phylogenies were calculated utilizing RAXML (v.8.2.9; -f a, -x 12 345, -p 12345, -# 100, -m PROTCATJTT).

Plant growth conditions

Duckweed fronds were propagated by transferring three mother fronds to a new well containing fresh media every 3–4 wk. Plants were grown on Schenk and Hildebrandt basal salt media (S6765-10L, 0.8% agarose, pH 6.5; Sigma-Aldrich) in six-well plates and then placed in a growth chamber set to 23°C with a diurnal cycle of 16 h : 8 h, light (75 μmol) : dark.

Pathogen inoculation

Bacterial colonies were grown in Luria Broth (LB) media supplemented with appropriate antibiotics (10 μg ml^{-1}; kanamycin (Km), 50 μg ml^{-1}; rifampicin (Rif), 50 μg ml^{-1}; spectinomycin (Sp)) overnight at 28°C in a shaking incubator (20.5 g). Pathogens used in this study included: *P. syringae* pv *tomato* DC3000 GFP (Matthysse *et al.*, 1996; Mudgett & Staskawicz, 1999), *P. syringae* pv *tomato* DC3000 *cma* (Sreedharan *et al.*, 2006), *P. syringae* pv *tomato* DC3000 *hrcC* (Mudgett & Staskawicz, 1999), *P. fluorescens* N2C3 (DSM 106121; Parte *et al.*, 2020), *P. syringae* B7281 (Feil *et al.*, 2005), *P. syringae* pv *glycinea* race 4 (Staskawicz *et al.*, 1987), *P. syringae* pv *tabaci* 11528 (Institute of Medicine (US) Committee on Resource Sharing *et al.*, 1996), *P. syringae* pv *maculicola* (Davis *et al.*, 1991), *X. euvesicatoria* (Roden *et al.*, 2004), *X. gardneri* (Schwartz *et al.*, 2017), *X. perforans* (Bophela *et al.*, 2019), and *X. translucens* (Peng *et al.*, 2016). All strains were plated on Rif; *P. syringae* pv *tomato* DC3000 on Rif/Km and *P. syringae* pv *tomato* DC3000 *cma* on Rif/Km/Sp. Liquid culture was centrifuged (3000 ***g***, 15 min). The pellet was resuspended in 10 mM magnesium chloride ($MgCl_2$), the optical density measured at a wavelength of 600 nm (OD_{600}) was determined, and the infiltration solution was diluted to a final standard high inoculum of $OD_{600} = 0.1$, equivalent to 1×10^8 cells of *Pst* DC3000. Then 500 μl of $OD_{600} = 0.1$ solution was pipetted on to three duckweed fronds per well. The plate was then returned to the incubator or placed in vacuum (0.8 PSI) for 10 min.

For growth curves, bacterial cells were resuspended at 1×10^8 colony-forming unit (CFU) ml^{-1}, $OD_{600} = 0.1$ in 10 mM $MgCl_2$. The inoculum was diluted to a standard low inoculum with a final concentration of 1×10^5 CFU ml^{-1}. Each well was inoculated with 500 μl of treatment, followed by vacuum infiltration (0.8 PSI) for 10 min. For each timepoint 1 cm^2 of fronds was sampled in 150 μl $MgCl_2$ and glass beads, then homogenized by a biospec mini-beadbeater (2000 rpm, vital distance 3.175 cm). Serial dilutions were made and plated on selective media. Two days after plating, colonies were counted.

Microscopy

For microscopy of duckweed treated with bacteria, flood inoculation with 500 μl solutions $OD_{600} = 0.1$ were used. Whole fronds were staged in water on slides and covered with a glass coverslip. The slides were imaged on a Zeiss 710 LSM confocal microscope (Zeiss) with either the 20× (water), 63× (oil) or 100× (oil) objectives. To image bacteria on duckweed fronds, they were stained with 10 μl of 1× Syto™ BC Green Fluorescent Nucleic Acid Stain (S34855; Thermo Scientific, Waltham, MA, USA). Duckweed fronds treated with SA were imaged on an Olympus SZX12 stereo microscope.

Hormone supplementation

Coronatine (C8115-1MG; Sigma-Aldrich) powder was dissolved in 100% dimethyl sulfoxide (DMSO) to create a 200 μM ml^{-1} stock that was then diluted to 3 and 0.3 μM in double-distilled water (ddH_2O). Salicylic acid (SA) BioXtra ≥ 99.0% (S5922-100G; Sigma-Aldrich) was diluted in water to concentrations of 2, 0.4 and 0.2 mM. Buffer solution used was the same as the solvent for the treatment. Individual wells of 6 or 12 well plates containing three duckweed fronds were inoculated with 500 or 250 μl of phytohormone solution, respectively. Phytohormone treatments were applied just before pathogen treatment.

RNA-Seq analysis

Inoculations were conducted as outlined earlier using standard high bacterial inoculum 1×10^8 CFU ml^{-1}. At 30 min, 1 h, 6 h and 12 h after inoculation, fronds from the same well were transferred to tubes containing 1.5 ml RNA later and frozen in liquid nitrogen. RNA was extracted using Qiagen RNAeasy plant kit (74903; Qiagen) and samples with a RNA integrity number score of > 8.0 (Agilent Bioanalyzer 2100 performed by QB3-UC Berkeley, Berkeley, CA, USA) were used for library preparation. Library construction and sequencing were performed by Novogene (Sacramento, CA, USA) using NEBNext Ultra II RNA library prep by Illumina (E7770; Illumina, San Diego, CA, USA) and an Illumina Novaseq 6000 S4. After sequencing, reads were demultiplexed using Illumina indices and a quality control (QC) check removed 'N' containing, low quality, and adapter-related reads. Upon receiving the data from Novogene, an initial QC of reads was performed with FastQC (Andrews, 2010). Reads were then mapped to the *S. polyrhiza* v.2 genome using Hisat2 (Kim *et al.*, 2015). Read coverage tables were computed using Stringtie (Pertea *et al.*, 2015) and differential gene expression analysis was carried out using edgeR (Dai *et al.*, 2014). Genes were considered differentially expressed if they met the criteria $|\log_2 FC| > 1$, FDR < 0.05 (FC, fold change; FDR, false discovery rate). For a detailed list of commands see: https://github.com/erin-baggs/DuckweedRNA. Outliers were removed by visual inspection; the edgeR count tables were plotted as PlotMDS method $\log_2 FC$ and BCV (Figs S1–S4). Samples were removed if they alone were causing most of the variance on a dimension leading to all other samples clustered into a corner. Then, if one sample of a treatment was grouping with samples of an opposing treatment, gene expression was analyzed to check whether the sample's expression pattern may have been the result of cross contamination. If the expression was inconsistent with at least three other replicates from the treatment group it belonged to, the sample was removed. Replicates removed from *S. polyrhiza* analysis included B3, B20, B19, P21, B34, P114. The replicates B15, B20, P39, P70, H80, B94, P103 and H115 were removed from *L. punctata* analysis.

Orthofinder (Emms & Kelly, 2019) was used to identify orthogroups between *A. thaliana* and duckweeds. *Arabidopsis thaliana* gene identifiers of marker genes were then used to extract the gene identifiers of duckweed homologs. The *S. polyrhiza* and *A. thaliana* homologous relationships were then cross-referenced by comparing to Phytozome protein homologs. Phytozome was then used to infer *O. sativa* homologs. The differential expression of the duckweed homologs to *A. thaliana* marker genes was extracted from edgeR data and plotted in R genevestigator (https://genevestigator.com; Hruz *et al.*, 2008) was used to identify the differential expression of *A. thaliana* homologs to duckweed upregulated genes in two public Affymetrix Arabidopsis ATH1 genome array (AtGenExpress: ME00331 (Kemmerling *et al.*, 2011) and GEO: GSE5520 (Thilmony *et al.*, 2006)) a third array was used to investigate ABA response (Array Express: E-MEXP-2378 (Umezawa *et al.*, 2010)). The differential expression *O. sativa* homologs to duckweed conserved pathogen upregulated genes was extracted from the EBI Expression atlas (Athar *et al.*, 2019).

Results

Lemnaceae condensed many immune signaling components and expanded the MiAMP1 protein family

To understand how immune genes have diverged within the Lemnaceae, we utilized publicly available genomes of *S. polyrhiza* (Wang *et al.*, 2014) and *W. australiana* (Michael *et al.*, 2020). Additionally, we assembled and annotated the genome of *L. punctata* clone 5635 (Table S1), which allowed us to catalog the presence and absence variation across three duckweed genera (Fig. 1a; Table S3). Consistent with previous findings *EDS1*, *PAD4*, and *RNLs* were absent across the Lemnaceae (Lapin *et al.*, 2019; Baggs *et al.*, 2020; Michael *et al.*, 2020). To estimate the timing of the EDS1 pathway loss, we used the closest related species to duckweeds with an available genome, giant Taro (*C. esculenta*; Yin *et al.*, 2021). Taro has the *EDS1* pathway (Fig. 1a), suggesting that the loss of these genes in Lemnaceae occurred after their divergence from Taro 104–117 Ma (Kumar *et al.*, 2017). The identification of several MiAMP1 genes in Taro (Fig. 1b) suggests the expansion of MiAMP1 proteins can occur independently of the loss of EDS1. Without greater depth of sampling of the Araceae family and sister lineages it remains unclear if MiAMP1 expansions are independent or a single expansion event.

To understand the extent of the immune signaling pathways divergence across Lemnaceae, we surveyed the presence of 24 protein families that have a known role in plant disease defense and pre-date the monocot and dicot divergence. All 24 protein families selected were present in *S. polyrhiza* (Tables S3, S4; Figs S5–S7). Though gene families associated with immunity were often retained in the Lemnaceae, we noticed a reduction in copy number, like NLRs (Figs 1b, S7; Table S3). Only three NB-ARC domain-containing proteins are present in *W. australiana* (Michael *et al.*, 2020): two of contain only an NB-ARC and the other is a TNP whose conservation is consistent with TNPs being EDS1 independent (Johanndrees *et al.*, 2021). *Wolffia australiana* has retained many other immune components. While we identified no orthologs of *Pathogenesis related* 4 (*PR4*), *SOBIR1* and *BAK1 interacting receptor 1* (*BIR1*) in *W. australiana*, they were present in *L. punctata* and *S. polyrhiza* (Fig. 1b; Table S3). Our

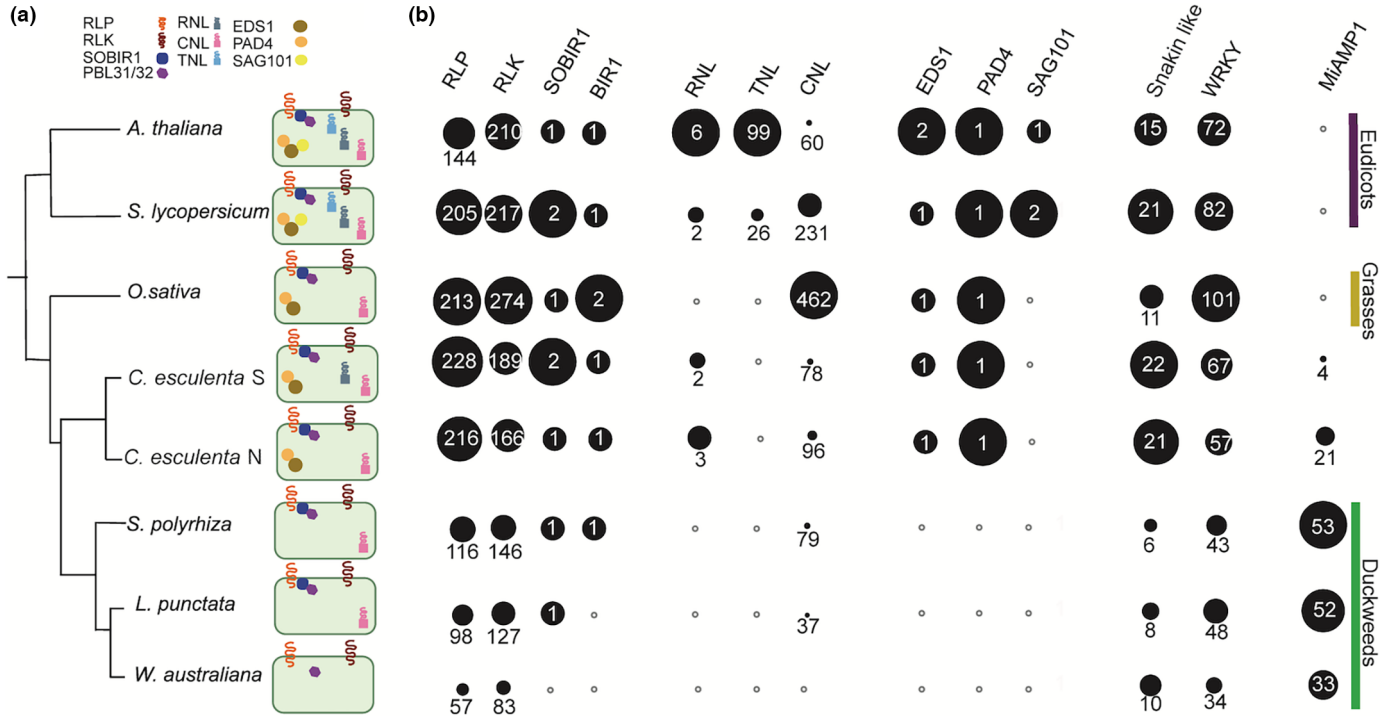

Fig. 1 Copy number variation of conserved angiosperm immune signaling components. (a) Phylogenetic relationship of duckweeds to other representative angiosperms and depiction of presence of signaling components. If components were not identified by ORTHOFINDER, reciprocal BLASTP, and TBLASTN, the representative symbol was not displayed in the cell. (b) The size of circles within each column are proportional to the highest copy number of that gene family in a given species, the copy number is denoted in white text. White circles with a gray outline indicate no members of that gene family were identified.

observations indicate that immune pathways have undergone varying degrees of gene loss across the duckweed genera.

Despite the trend towards reductionism of immune signaling components in the Lemnaceae, we identified high copy numbers of MiAMP1 domain-containing proteins. It has previously been shown that antimicrobial proteins in general are expanded in *S. polyrhiza* 7498 (An *et al.*, 2019). Phylogenies of Lemnaceae MiAMP1 proteins show lineage specific expansions and rapid birth and death (Fig. S8) suggesting that selection pressures may be favoring their diversification.

Duckweed species show variable symptoms upon *Pseudomonas* and *Xanthomonas* challenge

Since Lemnaceae species lack the EDS1 pathway, it was unclear how they would respond to bacterial pathogen infection. We challenged *S. polyrhiza*, *L. punctata*, and *W. australiana* to a panel of common *Pseudomonas* and *Xanthomonas* plant pathogens with a standard high bacterial inoculum (1×10^8 CFU ml^{-1}; Fig. 2a). We observed variability among replicates in the susceptibility and resistant phenotypes (Dataset S1; 2b) which is consistent with quantitative resistance. The variability was observed when experiments were started with a single (Fig. S9) or three mother fronds (all other experiments). We identified a few virulent pathogens that produced similar symptoms across all hosts (*X. gardneri*, *P. syringae* pv *tabaci*) while others caused distinct symptoms on a given host species. The most common disease symptoms were chlorosis and reduced growth rate. Surprisingly, despite having fewer NLRs and lacking *SOBIR1* and *BIR1*, the growth of *W. australiana* upon pathogen infection was often less stunted than that of other duckweed species.

For further experiments, we focused on *P. syringae* pv *tomato* DC3000 (*Pst* DC3000) and *P. syringae* pv *syringae* B728a (*Pss* B728a) as there are known virulence factors, large resources of mutants, and the severity of disease symptoms caused varied across duckweed species.

Pseudomonas syringae colonizes the substomatal cavity in *Spirodela polyrhiza* and infection is slowed in T3SS mutants

To characterize the pathology of *Pseudomonas* on duckweed, we used microscopy and bacterial genetics, taking advantage of the type III secretion deficient mutant *Pst* DC3000 *hrcC*.

Microscopy of flood inoculated *S. polyrhiza* fronds with standard high bacterial inoculum at 5 d post inoculation (dpi) showed *Pst* DC3000 populations were concentrated at the node (root and frond joint) and budding pockets (where daughter fronds emerge; Fig. S10). By 7 dpi, *Pst* DC3000 populations were observed at the stomata and within the substomatal cavity and mesophyll (Fig. 3a; Dataset S2). We also observed *Pst* DC3000 populations on root tissue at 7 dpi (Fig. 3b). *Pst* DC3000 *hrcC* infection resulted in surface populations on the frond at 5 dpi (Fig. S11a). Individual bacteria were present in the mesophyll (Fig. S11b) but no clear sub-stomatal populations. At 7 dpi like *Pst* DC3000 the *Pst* DC3000 *hrcC* populations were

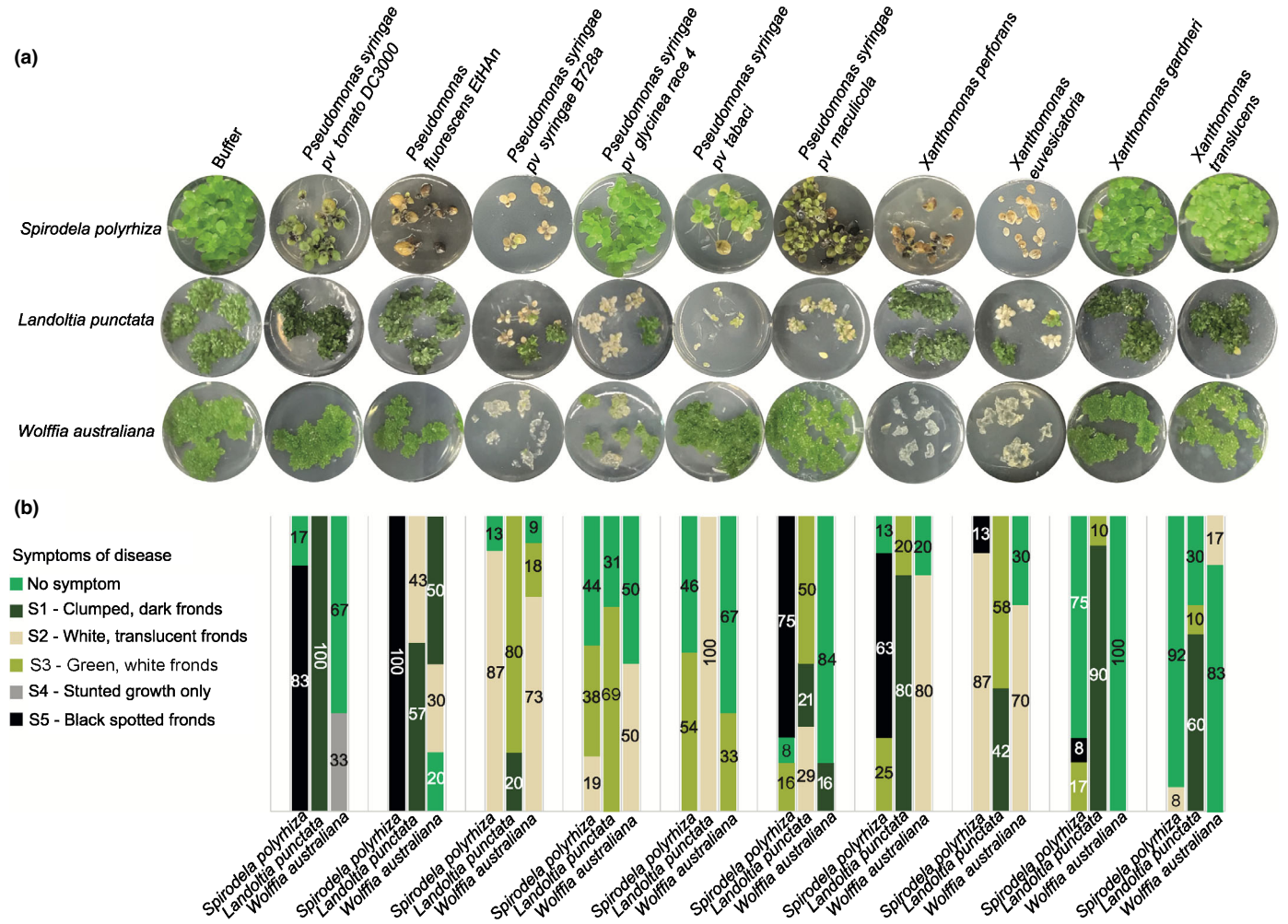

Fig. 2 Phenotypic response of duckweed species to bacterial pathogen treatments. (a). One replicate is shown per treatment (full experiment has been independently replicated three times, see Dataset S1; Table S5). Each well displays the most prevalent visual symptom of infection 3 wk after pathogen treatment of five frond clusters. (b) Bar graph showing the percentages of wells displaying each symptom among all replicates (Table S5). Colors of bars correspond to color legend of disease symptoms.

localized at the frond node (Fig. S11c) however, much smaller areas were colonized. The pattern of small surface populations and individual bacteria in the mesophyll remained the same at 5 and 7 dpi with *Pst* DC3000 *hrcC* (Fig. S11d,e). Together, our observations suggest that the visual symptoms of *Pseudomonas* on duckweed are a result of active bacterial infection. Therefore, the duckweed-*Pseudomonas* pathosystem constitutes a valuable model for understanding disease progression and EDS1-independent immune responses.

To advance our understanding of this pathosystem, we infiltrated *S. polyrhiza* plants with *Pst* DC3000 and *Pst* DC3000 *hrcC* with a low bacterial inoculum (1×10^5 CFU ml^{-1}) and monitored bacterial population growth overtime (Fig. 3c,d). The first black lesions were macroscopically visible at 3 dpi with *Pst* DC3000 and by day 5 we observed an increase in the size, number of lesions and proportion of affected fronds (Fig. 3c). Consistent with the dense populations at the budding pocket and node observed by microscopy, macroscopic black lesions observed were initially localized at the budding pocket and node. We observed no black lesions upon inoculation with *Pst* DC3000 *hrcC* at 3 or 5 dpi. In contrast, *L. punctata* infiltrated with *Pst* DC3000 or *Pss* B728a showed no macroscopic lesions even 5 dpi (Fig. 4a,b). Three weeks post inoculation, 5/8 replicates of *L. punctata* inoculated with *Pss* B728a had turned white and produced fewer daughter fronds than in other treatments. However, even at 4 wk post inoculation with *Pst* DC3000 we observed only a slightly darker coloration and clumping. *Pst* DC3000 *hrcC* did not cause any symptoms on *L. punctata* throughout the 3 wk post inoculation (Fig. S12).

Pst DC3000 and *Pst* DC3000 *hrcC* were able to proliferate inside *S. polyrhiza* (Fig. 3d). *Pst* DC3000 multiplied to similar levels as previously described in compatible interactions with wild-type *A. thaliana* (Katagiri *et al.*, 2002; Ishiga *et al.*, 2011; Velásquez *et al.*, 2017). However, we observed significantly fewer colony forming units of *Pst* DC3000 *hrcC* compared to *Pst* DC3000. This suggests that the virulence of *Pst* DC3000 on *S. polyrhiza* relies on the presence of effectors and the type III secretion system. In contrast, consistent with the lack of disease symptoms in *L. punctata* neither *Pst* DC3000 nor *Pst* DC3000 *hrcC* showed significantly different CFU counts at 5 dpi. Instead,

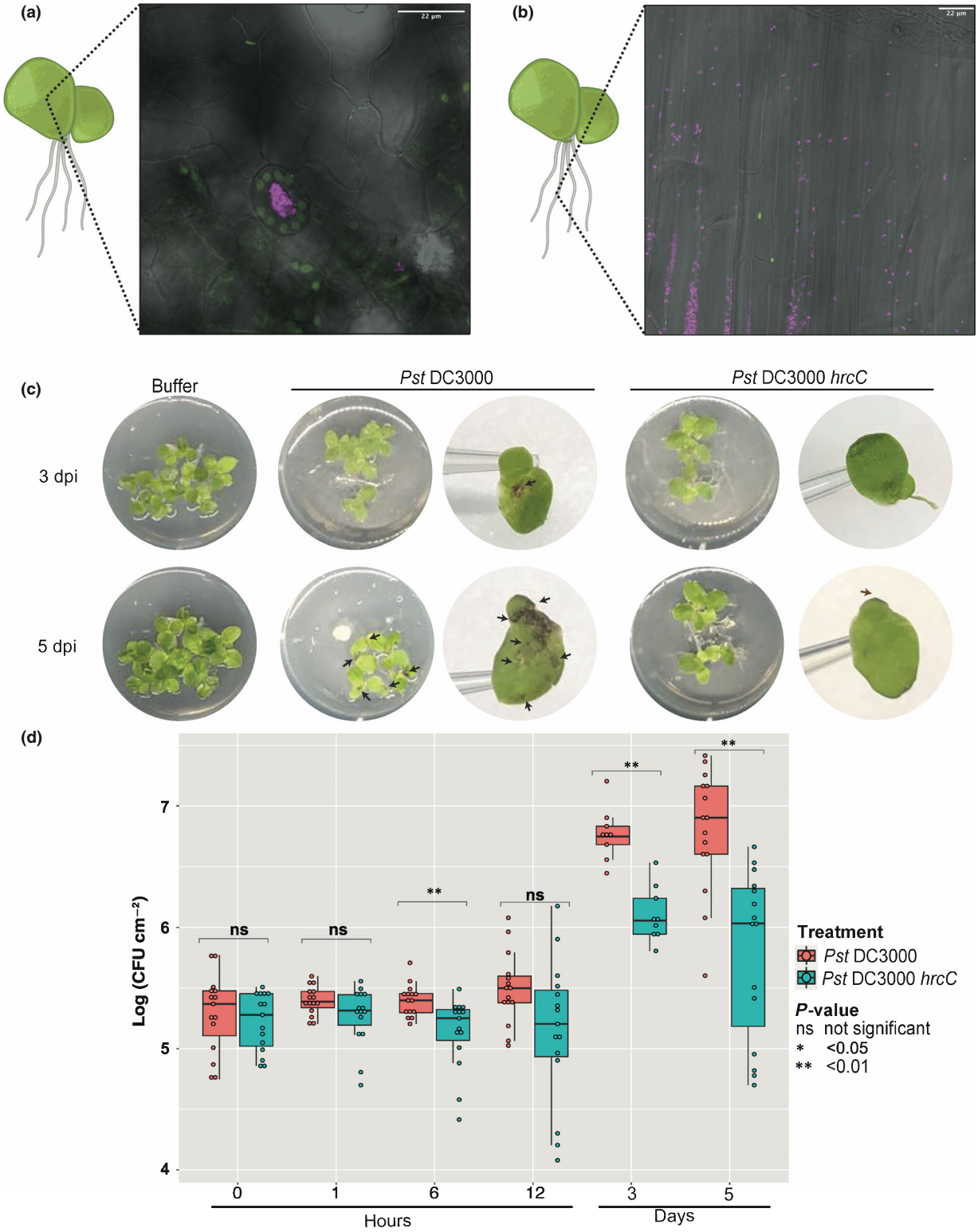

Fig. 3 *Pst* DC3000 infection of *Spirodela polyrhiza*. Confocal ×100 microscopy of *Spirodela polyrhiza* inoculated with *Pst* DC3000. False colors: pink – *Pst* DC3000, green – plastids, gray – transmitted light. (a) Frond surface with stomata in the center of frame. (b) Root tissue. (c) Images of duckweed fronds and symptoms at 3 and 5 d post inoculation (dpi) with *Pst* DC3000 and *Pst* DC3000 *hrcC*. The *Pst* DC3000 *hrcC* mutant lacks the type III secretion system used for deployment of effectors to the plant. Individual fronds were photographed on a 10 µl tip to indicate size of fronds. Arrows highlight areas where symptoms are present. (d) Box plot showing the number of colony-forming units (CFUs) of *Pst* DC3000 and *Pst* DC3000 hrcC at different time points on *Spirodela polyrhiza* fronds. The top horizontal line of each box represents the upper quartile followed by the median and lower quartile. The range extends between the smallest data point within the first quartile value subtract 1.5× the interquartile range and the largest data point within the third quartile value add 1.5× the interquartile range. Colored circles indicate individual data points. Mean-*t* statistic with Holm adjustment used to assess statistical difference between treatments.

both bacterial numbers remained at a level similar to those of *Pst* DC3000 *hrcC* in *S. polyrhiza* (Fig. 4c). Interestingly, although we saw no visible lesions on *L. punctata* 5 d after *Pss* B728a inoculation, the CFU counts were significantly higher than those of *Pst* DC3000 after 5 d. However, the CFU counts of *Pss* B728a in *L. punctata* and *Pst* DC3000 in *S. polyrhiza* were similar. Our

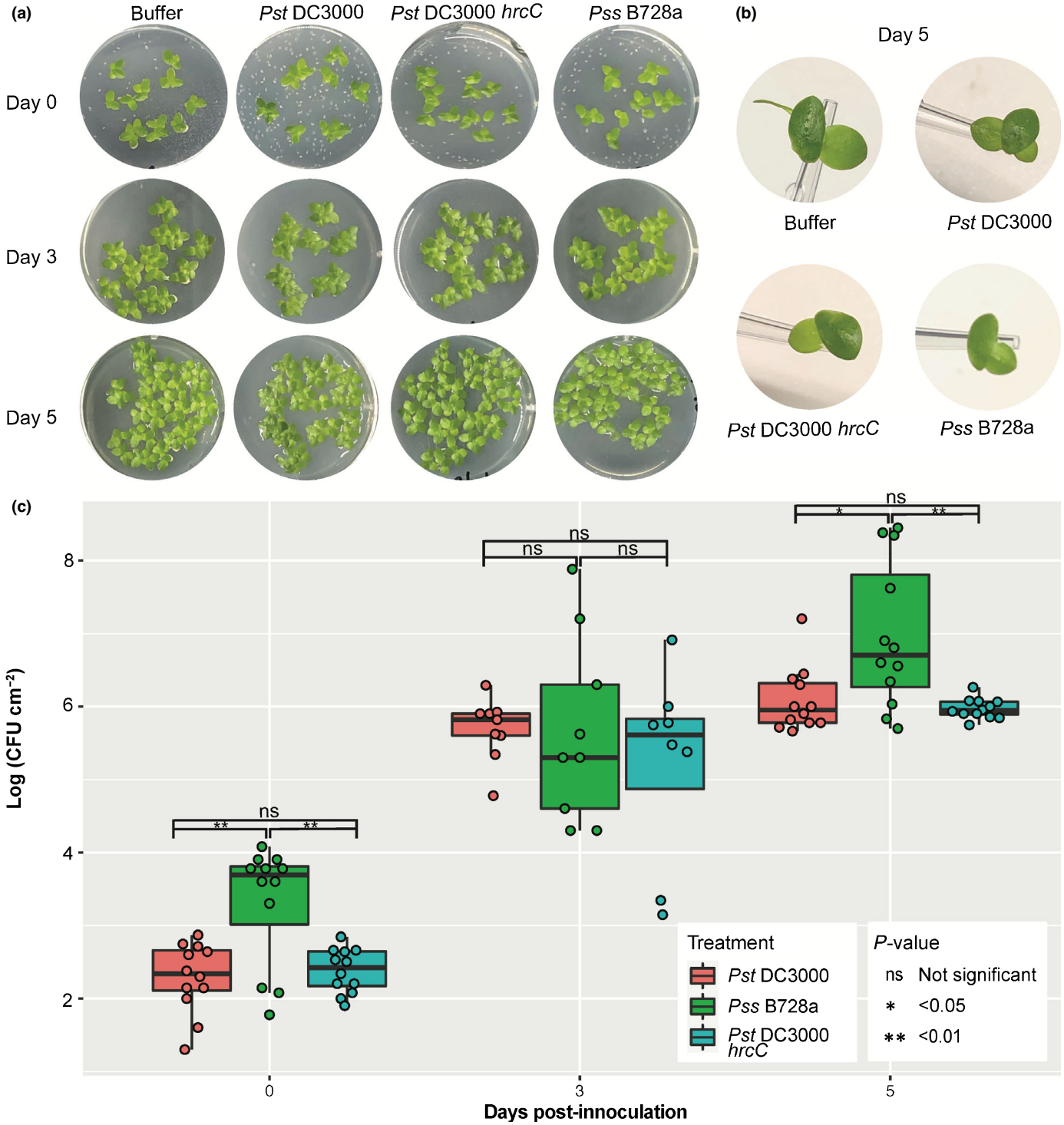

Fig. 4 *Pst* DC3000 infection of *Landoltia punctata*. (a) Images of *Landoltia punctata* fronds and symptoms during *Pst* DC3000, *Pst* DC3000 *hrcC* and *Pss* B728a. (b) Individual fronds were photographed on a 10 µl tip to indicate size of fronds. (c) Box plot showing the number of colony-forming units (CFUs) of *Pst* DC3000, *Pst* DC3000 *hrcC* and *Pss* B728a at different time points on *Landoltia punctata* fronds. The top horizontal line of each box represents the upper quartile followed by the median and lower quartile. The range extends between the smallest data point within the first quartile value subtract 1.5× the interquartile range and the largest data point within the third quartile value add 1.5× the interquartile range. Colored circles indicate individual data points. Mean-*t* statistic with Holm adjustment used to assess statistical difference between treatments.

results show that *Pseudomonas* pathogens *Pst* DC3000 and *Pss* B728a can proliferate in duckweed host and bacterial multiplication is affected by unknown host factors and by the type III secretion system for *S. polyrhiza*–*P*st DC3000 interaction.

Hormone treatment effects vary among Lemnaceae spp. and pathogen treatment

In response to biotrophy, plants upregulate the phytohormones SA (Cao *et al.*, 1994; Clarke *et al.*, 1998) and N-hydroxy pipecolic acid (NHP) through pathways dependent and independent of *EDS1* (Chen *et al.*, 2018). To suppress phytohormone responses, *Pst* DC3000 produces the toxin coronatine (Moore *et al.*, 1989; Mittal & Davis, 1995), a structural mimic of jasmonic acid (JA) which counteracts SA upregulation (Fonseca *et al.*, 2009; Wasternack & Xie, 2010). Since *Pst* DC3000 was virulent on *S. polyrhiza*, we investigated the role of phytohormones and toxins in the absence of *EDS1* through our duckweed pathosystem. The *Pst* DC3000 *cma* mutant is deficient in coronatine biosynthesis and causes mild symptoms on *S. polyrhiza*, marked by the absence of black lesions (Figs 5a, S13, S14). Addition of coronatine alone (0.3 μM) was sufficient to disfigure fronds, reduce growth, and induce the formation of turion resting bodies. The effect on growth and turion formation was stronger at higher concentrations of coronatine (3 μM). However, addition of coronatine on its own was not sufficient to recover symptoms of black lesions and white bleaching of fronds comparable to *Pst* DC3000 infection. The treatment of fronds with coronatine at the time of *Pst* DC3000 *cma* infection restored the black lesions to some extent, but the strain still did not induce white bleaching. Our results show that coronatines role in promoting pathogen virulence is conserved in duckweeds despite the absence of the SA promoting EDS1 pathway.

Given that a core function of the EDS1 pathway is to reinforce SA signaling by inducing several SA responsive genes (Jirage *et al.*, 1999; Bonardi *et al.*, 2011; Roberts *et al.*, 2013; Cui *et al.*, 2017); we were interested in how exogenous SA treatment of Lemnaceae would affect disease symptoms. Treatment of Lemnaceae with high levels of SA (2 mM) that are tolerated in *Arabidopsis* were phytotoxic to *S. polyrhiza* (Fig. S15). We therefore carried out experiments using 0.4 and 0.2 mM SA. At these lower concentrations in the absence of a pathogen, we observed dose-dependent frond disfiguration, growth reduction and an increase in turion formation in *S. polyrhiza*. *L. punctata* only showed growth reduction with 0.4 mM SA (Fig. S16). *S. polyrhiza* co-treated with SA and *Pst* DC3000 showed typical *Pst* DC3000-induced symptoms (Figs 5b, S17–S20). However, a small protective effect of SA was observed when *Pst* DC3000 appeared to be less virulent (Fig. S20). We hypothesize that the variation in virulence of *Pst* DC3000 on *S. polyrhiza* affects the ability of SA to restrict pathogen growth below a critical threshold. In the *L. punctata*–*Pss* B728a pathosystem, there was a clear protective effect of SA. Priming of *L. punctata* with SA resulted in loss of the chlorotic symptoms characteristic of the *Pss* B728a treated fronds (Figs 5c, S21, S22). The effect of SA priming on duckweed pathogen interactions appears to be influenced by pathogen strain and plant genotype and complicated by strong endogenous effects of SA on duckweed physiology.

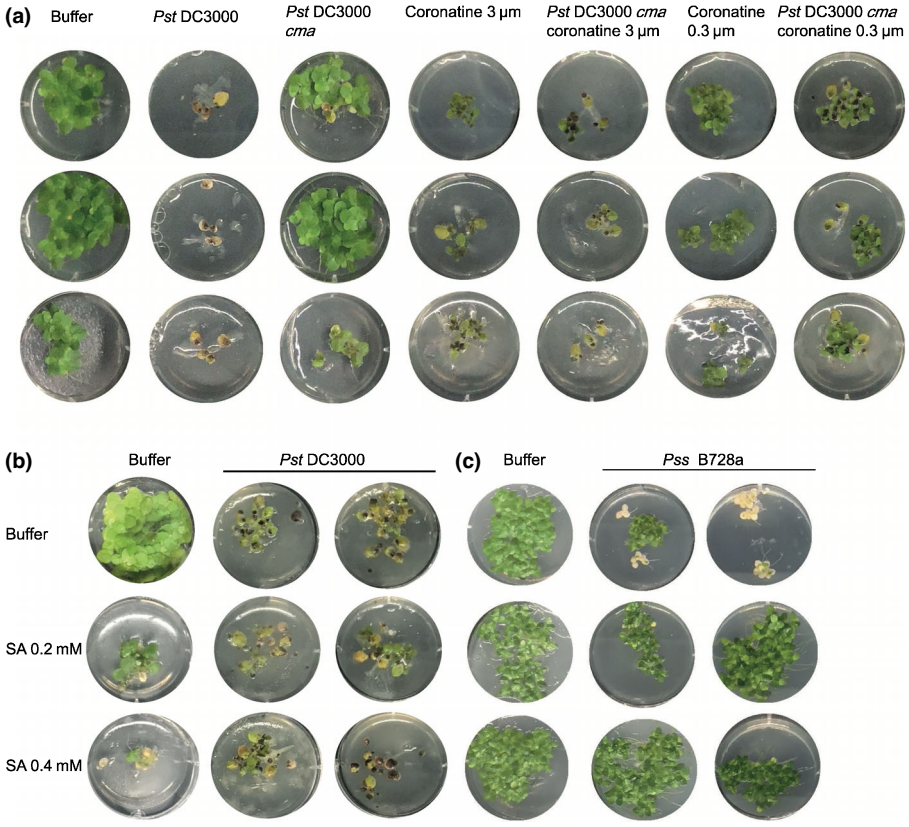

Fig. 5 The effects of hormone treatments on *Pst* DC3000 and *Pss* B728a disease symptoms. (a) Images of disease progression 3 wk after the treatment of three *Spirodela polyrhiza* fronds with different concentrations and combinations of coronatine and *Pst* DC3000 mutants (full experiment has been independently replicated three times, see Figs S13, S14). (b) Images of disease progression 3 wk after the treatment of five *S. polyrhiza* fronds with different concentrations and combinations of salicylic acid (SA) and *Pst* DC3000 (full experiment has been independently replicated four times, see Figs S17–S19). (c) Images of disease progression 3 wk after the treatment of five *Landoltia punctata* fronds with different concentrations and combinations of SA and *Pss* B728a treatment, *Pss* B728a was used rather than *Pst* DC3000 as it gives clearer visual symptoms in *L. punctata* (full experiment has been independently replicated three times, see Figs S21, S22).

Spirodela polyrhiza and *Landoltia punctata* mount transcriptional responses to *Pst* DC3000

Next, we investigated transcriptional response to *Pseudomonas* infection. Despite the absence of *EDS1*, RNA-Seq revealed a substantial transcriptional response as early as 30 min post infection (Figs 6a, S23; Datasets S3, S4). We first examined gene families that are differentially expressed upon pathogen treatment in other plant species: WRKY (Dong *et al.*, 2003), MiAMP1 (Fig. 6b; Adomas & Asiegbu, 2006; Adomas *et al.*, 2007), NB-ARC (Richard *et al.*, 2018), and JAZ domain-containing genes (Ishiga *et al.*, 2013; Fig. S24; Tables S6–S13). While we did not

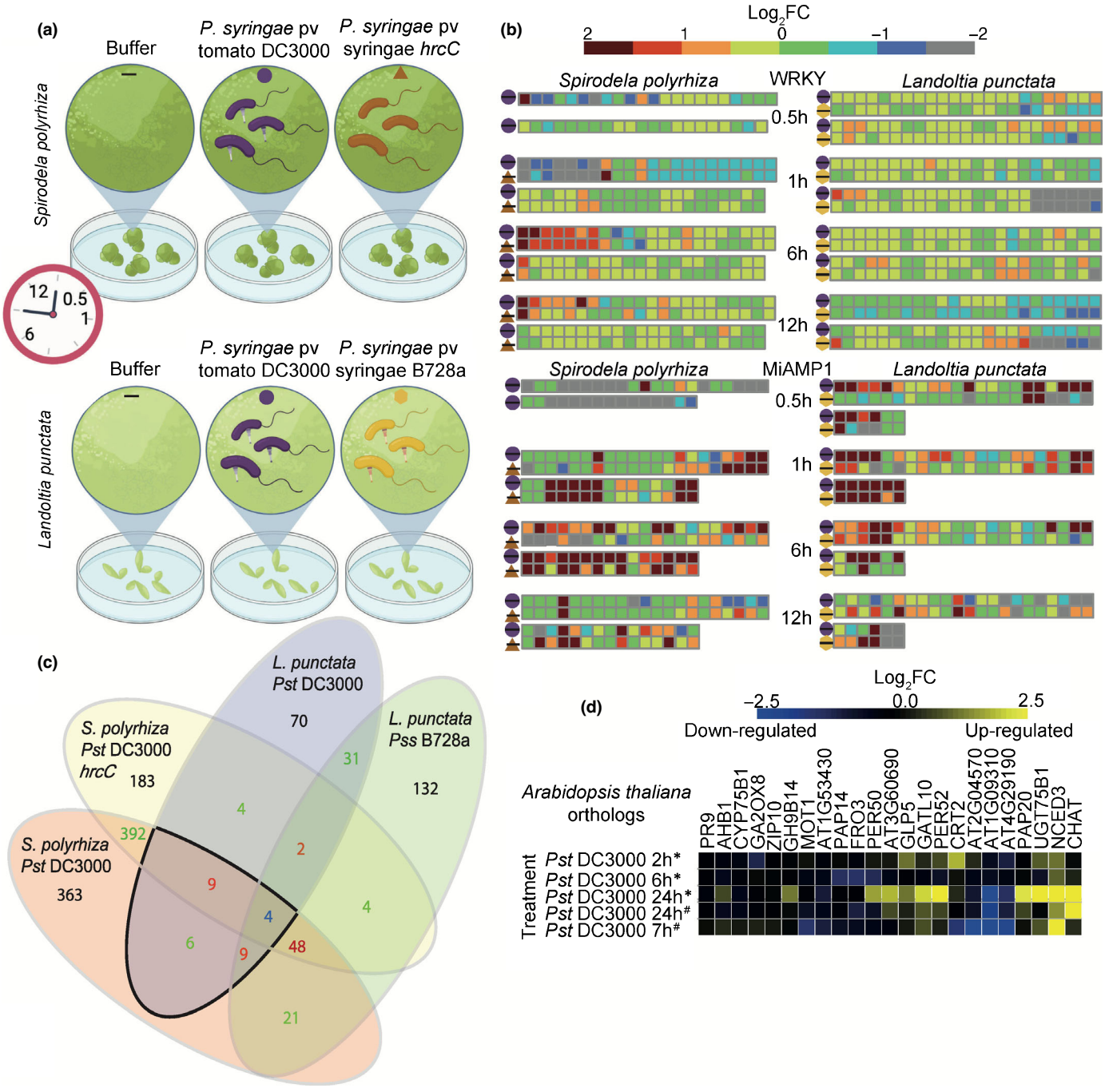

Fig. 6 Log_2-fold change (FC) of selected gene families following bacterial pathogen exposure of duckweeds. (a) Schematic of the sampling regime for RNA-sequencing (RNA-Seq) study. (b) Each square represents a gene with a given domain, the differential expression of the gene is shown by the color of the square. The treatment comparison is indicated by the shapes shown in (a). (c) Venn diagram of numbers of orthogroups that show differential expression ($log_2FC > 1$, false discovery rate (FDR) < 0.05) in multiple combinations of pathogen treatments and or across different species at any time point. (d) Microarray differential expression analysis of representatives from *Arabidopsis thaliana* Col-0 of those orthogroups with conserved upregulation upon *Pst* DC3000 in *Spirodela polyrhiza* and *Landoltia punctata*.

observe consistent upregulation $\log_2FC > 1$ of NB-ARC and WRKY domain-containing genes, MiAMP1 domain-containing genes were consistently upregulated over time in both duckweed species after pathogen treatment.

We hypothesized that there may be some orthologs of *A. thaliana* bacterial-response genes that are also upregulated in duckweed species upon bacterial infection. Among the 33 *S. polyrhiza* and 32 *L. punctata* genes considered homologous to *A. thaliana* bacterial-responsive genes (Boudsocq *et al.*, 2010; Bjornson *et al.*, 2021; Salguero-Linares *et al.*, 2021; Tables S2, S14; Fig. S25), we were able to identify five *S. polyrhiza* and five *L. punctata* gene orthogroups that were significantly upregulated upon pathogen treatment ($\log_2FC > 1$, FDR < 0.05; Table S15).

Given the suppression of *Pss* B728a symptoms in *L. punctata* upon SA treatment we hypothesized the reduced symptoms seen in *L. punctata* compared to *S. polyrhiza* after *Pst* DC3000 treatment may be due to greater upregulation of SA pathways in *L. punctata*. We investigated the differential expression of duckweed homologs of *A. thaliana* SA biosynthetic and regulated genes (Fig. S26a; Table S16). In *S. polyrhiza* and *L. punctata* we did not observe consistent upregulation of upstream SA biosynthesis genes and regulators (*ICS1*, *NPR1*, *SARD1*, *CBP60g*) or SA catabolism (*DMR6*; Fig. S26b; Tables S17, S18). However, in both duckweed species we saw consistent upregulation of PR1/PR2 -like genes which in *A. thaliana* are upregulated downstream of SA production. *L. punctata* also upregulates *WRKY40* homologs after pathogen treatment. Together this indicates that *A. thaliana* and duckweed pathogen transcriptional response pathways converge downstream of SA production and differences in SA signaling is unlikely to explain different disease outcomes between duckweed species.

To investigate which genes have conserved upregulation in *A. thaliana* and duckweeds, we created interspecific orthogroups with ORTHOFINDER (Emms & Kelly, 2019). Then, we identified orthogroups with members that were significantly differentially expressed in both duckweeds after *Pst* DC3000 treatment (Fig. 6c; Table S19; Dataset S5). For orthogroups with conserved upregulation in both duckweeds, we investigated if the *A. thaliana* homologs were similarly upregulated upon *Pst* DC3000 infection, using publicly available datasets (Figs 6d, S27). Among the *A. thaliana* homologs, eight genes showed consistent upregulation after *Pst* DC3000 treatment, including a superoxide dismutase *GERMIN-LIKE PROTEIN 5*. In contrast upon pathogen treatment, *PATHOGENESIS RELATED 9* (*PR9*) was upregulated in duckweeds but not in *A. thaliana*. There appears to be limited overlap in the transcriptional response to *Pst* DC3000 between *A. thaliana* and duckweeds. Interestingly, half of the orthogroups upregulated in response to bacterial infection, in duckweeds and Arabidopsis were hormone-regulated or biosynthetic genes suggesting a conserved role of hormones. As the immune pathways of monocots and dicots have diverged substantially, we looked at the differential expression of orthologs of the duckweed upregulated genes in rice across several pathogen treatments (Fig. S28; Table S20). Ten of 28 orthogroups upregulated in duckweeds were also upregulated in rice ($\log_2FC > 1.5$ across three treatments). Among these genes, five orthogroups included genes also upregulated in *A. thaliana*.

Finally, we identified genes upregulated and unique to duckweeds. Four orthogroups which showed conserved differential expression in both duckweed species do not have homologs in *A. thaliana* (Table S19) of these only two lacked homologs in rice. The two unique orthogroups were cytochrome P450 domain-containing genes. Cytochrome P450s are present in *A. thaliana* and *O. sativa* (Nelson *et al.*, 2004), but lack sequence conservation to those upregulated in duckweeds. MiAMP1 domain-containing genes are not present in *A. thaliana*. Although MiAMP1 proteins were upregulated across timepoints in both duckweeds, orthogroups containing these proteins did not meet the criteria for conserved upregulation. Since duckweed species do not show a qualitative but a quantitative resistance, we hypothesize that such resistance mechanisms could involve MiAMP1 proteins and cytochrome P450s.

Discussion

We investigated the immune responses of Lemnaceae whose immune pathways have evolved for *c.* 110 million years in the absence of *EDS1*, a hub for signaling and crosstalk in plant immune system. Whilst the loss of *EDS1* predates the divergence of Lemnaceae, only *W. australiana* has lost the MTI signaling components SOBIR1-BIR1 (Gao *et al.*, 2009; Liebrand *et al.*, 2013; Albert *et al.*, 2015; van der Burgh *et al.*, 2019). Previous work illustrates RLP-SOBIR1 dependence on EDS1 and PAD4 in *A. thaliana* (Pruitt *et al.*, 2021). Despite the loss of *SOBIR1*, compared to other Lemnaceae, *W. australiana* did not have enhanced susceptibility to the bacterial pathogens tested. Given available resources, we began developing and characterizing the pathosystem of *S. polyrhiza* and *L. punctata* interactions with *Pst* DC3000 and *Pss* B728a. Transcriptional and bacterial mutant assays revealed the importance of phytohormones in their response to pathogens; however, differential expression of bacteria responsive *A. thaliana* orthologs was rarely observed. Furthermore, we show that there is a high copy-number and upregulation upon pathogen infection of MiAMP1 domain-containing proteins in Lemnaceae.

Duckweeds exist with complex bacterial communities similar to the terrestrial leaf microbiome (Acosta *et al.*, 2020). Several duckweed-associated bacteria have growth promoting effects (O'Brien *et al.*, 2020). To understand disease resistance of Lemnaceae to pathogenic bacteria, we screened a range of bacterial pathogens to identify a model pathosystem. Our data shows differences in macroscopic symptoms across Lemnaceae species upon treatment with the same pathogen. Variability was present between fronds within the same treatment well, suggesting there may be environmental and population level factors affecting the outcome of infection. The variability in susceptibility across time points is consistent with quantitative resistance. The invasive nature of duckweeds and numerous healthy populations in the environment raises the questions of how environmental factors may contribute to their quantitative disease resistance. Furthermore, because duckweeds primarily reproduce clonally, have low mutation rates (Sandler *et al.*, 2020) and effective recombination (Ho *et al.*, 2019), there is limited opportunity for immune proteins to

diversify, which is required for generating new resistance specificities. The rather unique combination of duckweeds life-history traits of fast-growth, clonal reproduction, reduced morphological complexity and aquatic habitat could influence mechanisms of resistance. In a freshwater habitat, the frequency of contact with MAMPs and microbes likely differs from soil and could affect the balance of the energy trade-off between growth and defense (Huot *et al.*, 2014).

The use of bacterial mutant *Pst* DC3000 *hrcC* revealed the type-III secretion system can promote virulence of *Pst* DC30000 on *S. polyrhiza*, similar effects have been observed in *A. thaliana* (Hauck *et al.*, 2003; Xin *et al.*, 2016; Huot *et al.*, 2017). Furthermore, our results suggest that virulence of *Pst* DC3000 on *S. polyrhiza* relies on manipulation of host phytohormone pathways through the production of the JA mimic coronatine, similar to in *A. thaliana* (Moore *et al.*, 1989; Mittal & Davis, 1995). In contrast, *L. punctata* appears to have a stronger quantitative resistance response to *Pst* DC3000 even in the presence of coronatine. Despite the lack of conservation of the EDS1 pathway in *S. polyrhiza* and *L. punctata*, phytohormones and bacterial toxins remain key mediators of plant–bacterial infection. The reduction of MTI/ETI components in duckweeds opens questions of how duckweeds pathogens evolve; would reduction in effector repertoire be selected due to a reduced pressure for MTI/ETI suppression or would effectors further expand without ETI systems to activate.

Consistent with the variation in phenotypes upon bacterial inoculations, there was a lot of variation that was not explained by pathogen treatment between transcriptomes of duckweed biological replicates. The high variability could be a result of the asynchronous developmental stages of fronds, the quantitative nature of the resistance that we observed within the same population of duckweed or a combination of factors. The use of whole plant tissues likely diluted the signal of differential gene expression. In future studies, single cell transcriptomics might be informative for studying quantitative resistance phenotypes. Despite the variability, our transcriptomic analysis revealed that among the genes consistently differentially expressed after *Pseudomonas* treatment were MiAMP1-domain-containing proteins. We hypothesize MiAMP1-domain proteins maybe upregulated as a nonspecific response to infection, that protects against some but not all pathogens. Such consistent upregulation invites the speculation that they could function against pathogens similarly to MiAMP1 from Macadamia (McManus *et al.*, 1999; Stephens *et al.*, 2005) which was shown to have anti-microbial activity against gram-positive bacteria and fungal pathogens (Marcus *et al.*, 1997; Kazan *et al.*, 2002; Stephens *et al.*, 2005). Thus, duckweed MiAMP1 proteins warrant further investigation against some of the known fungal and oomycetes pathogens of duckweed (Fisch, 1884; Gaumann, 1928; Vanky, 1981; Rejmankova *et al.*, 1986; Flaishman *et al.*, 1997; Czeczuga *et al.*, 2005; Brand *et al.*, 2021). Other commonly differentially expressed protein families were associated with cytochrome P450s and phytohormones, indicating that specialized metabolites may have an important role in duckweeds infection response. Together, our data highlights that, despite the absence of *EDS1*, there are conserved areas of immune response pathways across plant species, such as phytohormones and secondary metabolism. Perhaps the reduced reliance on NLR–EDS1 pathways in duckweeds released selective constraints allowing avoidance of the typical plant–NLR vs pathogen–effector arms races and facilitating amplification of alternate immune strategies.

Duckweeds are an exciting system for research into plant immunity. They provide a reduced redundancy system in terms of both gene copy number and pathways present. In addition, their rapid lifecycle of just 34 h (Michael *et al.*, 2020), small size and susceptibility to model pathogens make them the perfect system for high-throughput experimentation. The genomic and genetic resources are also developing at a rapid pace (Wang *et al.*, 2014; Michael *et al.*, 2017, 2020; Hoang *et al.*, 2018; An *et al.*, 2019; Ho *et al.*, 2019; Xu *et al.*, 2019; Harkess *et al.*, 2021) and a range of transformation protocols (Ko *et al.*, 2011; J. Yang *et al.*, 2018; G-L. Yang *et al.*, 2018; Liu *et al.*, 2019; Acosta *et al.*, 2021; Chanroj *et al.*, 2021). Many interesting questions remain to be answered including how duckweed plants can thrive in a wide range of environments despite being highly susceptible to bacterial phytopathogens in the laboratory setting. One hypothesis is that duckweeds may be using means of disease protection that are inherently absent in the laboratory due to the way duckweeds are propagated. This may include microbiome-mediated disease protection, small peptide defense molecules such as MiAMP1s or chemical defense strategies. A combination of genetics, molecular biology and metabolomic approaches will be needed to address these hypotheses.

Acknowledgements

The authors would like to thank Dr Denise Schichnes and Dr Steven Ruzin for their expert advice and help with confocal microscopy. Research reported in this publication was supported in part by the National Institutes of Health (NIH) S10 program under award number 1S10RR026866-01. The content is solely the responsibility of the authors and does not necessarily represent the official views of the NIH. Many thanks to China Lunde for propagation of duckweed during the pandemic and to Dr Wilfried Haerty and the members of the Krasileva laboratory for helpful discussions. The authors acknowledge funding from the Biotechnology and Biological Sciences Research Council (BBSRC), part of UK Research and Innovation, Core Capability Grant BB/CCG1720/1 and the work delivered via the Scientific Computing group, as well as support for the physical HPC infrastructure and data center delivered via the NBI Computing infrastructure for Science (CiS) group. This research has been supported by the Gordon and Betty Moore Foundation (8802), Innovative Genomics Institute, and the NIH Director's Award (052239-002).

Author contributions

ELB performed genomic/transcriptomic presence absence analysis, growth curves, hormone assays, microscopy and RNA-Seq analysis. MBT and ELB performed the screen of phytopathogens across duckweed species and RNA extractions. BWA and TPM

performed DNA extraction, genome assembly and annotation of *L. punctata* 5635 genome. ELB and KVK designed the study. ELB prepared figures and wrote the full manuscript draft; all authors have read and approved the final version of the manuscript.

ORCID

Brad W. Abramson https://orcid.org/0000-0003-0888-3648
Erin L. Baggs https://orcid.org/0000-0003-3076-9489
Ksenia V. Krasileva https://orcid.org/0000-0002-1679-0700
Todd P. Michael https://orcid.org/0000-0001-6272-2875
Meije B. Tiersma https://orcid.org/0000-0003-0530-9640

Data availability

Sequencing reads for *S. polyrhiza* and *L. punctata* RNA-Seq can be found at the respective NCBI BioProjects PRJNA808038 and PRJNA801691. The *L. punctata* 5635 genome can be found on CoGe accession ID: 63585. Scripts for analysis presented in the manuscript can be found on the github repository https://github.com/erin-baggs/DuckweedRNA. Z-stack of *Pst* DC3000 infection of *Spirodela polyrhiza* is available from Zenodo doi: 10.5281/zenodo.5639580.

References

Abramson BW, Novotny M, Hartwick NT, Colt K, Aevermann BD, Scheuermann RH, Michael TP. 2021. The genome and preliminary single-nuclei transcriptome of *Lemna minuta* reveals mechanisms of invasiveness. *Plant Physiology* **188**: 879–897.

Acosta K, Appenroth KJ, Borisjuk L, Edelman M, Heinig U, Jansen MAK, Oyama T, Pasaribu B, Schubert I, Sorrels S *et al.* 2021. Return of the Lemnaceae: duckweed as a model plant system in the genomics and postgenomics era. *Plant Cell* **33**: 3207–3234.

Acosta K, Xu J, Gilbert S, Denison E, Brinkman T, Lebeis S, Lam E. 2020. Duckweed hosts a taxonomically similar bacterial assemblage as the terrestrial leaf microbiome. *PLoS ONE* **15**: e0228560.

Adomas A, Asiegbu FO. 2006. Analysis of organ-specific responses of *Pinus sylvestris* to shoot (*Gremmeniella abietina*) and root (*Heterobasidion annosum*) pathogens. *Physiological and Molecular Plant Pathology* **69**: 140–152.

Adomas A, Heller G, Li G, Olson A, Chu T-M, Osborne J, Craig D, van Zyl L, Wolfinger R, Sederoff R *et al.* 2007. Transcript profiling of a conifer pathosystem: response of *Pinus sylvestris* root tissues to pathogen (*Heterobasidion annosum*) invasion. *Tree Physiology* **27**: 1441–1458.

Albert I, Böhm H, Albert M, Feiler CE, Imkampe J, Wallmeroth N, Brancato C, Raaymakers TM, Oome S, Zhang H *et al.* 2015. An RLP23–SOBIR1–BAK1 complex mediates NLP-triggered immunity. *Nature Plants* **1**: 15140.

Alhoraibi H, Bigeard J, Rayapuram N, Colcombet J, Hirt H. 2019. Plant immunity: the MTI-ETI model and beyond. *Current Issues in Molecular Biology* **30**: 39–58.

Ali S, Ganai BA, Kamili AN, Bhat AA, Mir ZA, Bhat JA, Tyagi A, Islam ST, Mushtaq M, Yadav P *et al.* 2018. Pathogenesis-related proteins and peptides as promising tools for engineering plants with multiple stress tolerance. *Microbiological Research* **212-213**: 29–37.

An D, Zhou Y, Li C, Xiao Q, Wang T, Zhang Y, Yongrui W, Li Y, Chao D-Y, Messing J *et al.* 2019. Plant evolution and environmental adaptation unveiled by long-read whole-genome sequencing of *Spirodela*. *Proceedings of the National Academy of Sciences, USA* **116**: 18893–18899.

Andrews S. 2010. *FastQC: a quality control tool for high throughput sequence data (Online).* [WWW document] URL https://www.bioinformatics.babraham.ac.uk/projects/fastqc/ [accessed 8 November 2021].

Athar A, Füllgrabe A, George N, Iqbal H, Huerta L, Ali A, Snow C, Fonseca NA, Petryszak R, Papatheodorou I *et al.* 2019. ArrayExpress update – from bulk to single-cell expression data. *Nucleic Acids Research* **47**: D711–D715.

Atibalentja N, Keating K, Fields CJ. 2019. *Taro Niue genome assembly and annotation.* (dataset) 10.31.2019. NCBI. [WWW document] URL https://www.ncbi.nlm.nih.gov/bioproject/PRJNA328799 [accessed 6 January 2022].

Baggs E, Dagdas G, Krasileva KV. 2017. NLR diversity, helpers and integrated domains: making sense of the NLR IDentity. *Current Opinion in Plant Biology* **38**: 59–67.

Baggs EL, Grey Monroe J, Thanki AS, O'Grady R, Schudoma C, Haerty W, Krasileva KV. 2020. Convergent loss of an *EDS1/PAD4* signaling pathway in several plant lineages reveals coevolved components of plant immunity and drought response. *Plant Cell* **32**: 2158–2177.

Bailey PC, Schudoma C, Jackson W, Baggs E, Dagdas G, Haerty W, Moscou M, Krasileva KV. 2018. Dominant integration locus drives continuous diversification of plant immune receptors with exogenous domain fusions. *Genome Biology* **19**: 23.

Bankevich A, Nurk S, Antipov D, Gurevich AA, Dvorkin M, Kulikov AS, Lesin VM, Nikolenko SI, Pham S, Prijbelski AD *et al.* 2012. SPADES: a new genome assembly algorithm and its applications to single-cell sequencing. *Journal of Computational Biology* **19**: 455–477.

Barson G, Griffiths E. 2016. SEQTOOLS: visual tools for manual analysis of sequence alignments. *BMC Research Notes* **9**: 39.

Bjornson M, Pimprikar P, Nürnberger T, Zipfel C. 2021. The transcriptional landscape of *Arabidopsis thaliana* pattern-triggered immunity. *Nature Plants* **7**: 579–586.

Bog M, Appenroth K-J, Sowjanya Sree K. 2019. Duckweed (Lemnaceae): its molecular taxonomy. *Frontiers in Sustainable Food Systems* **3**: 117.

Bonardi V, Tang S, Stallmann A, Roberts M, Cherkis K, Dangl JL. 2011. Expanded functions for a family of plant intracellular immune receptors beyond specific recognition of pathogen effectors. *Proceedings of the National Academy of Sciences, USA* **108**: 16463–16468.

Bophela KN, Venter SN, Wingfield MJ, Duran A, Tarigan M, Coutinho TA. 2019. *Xanthomonas Perforans*: a tomato and pepper pathogen associated with bacterial blight and dieback of *Eucalyptus pellita* seedlings in Indonesia. *Australasian Plant Pathology* **48**: 543–551.

Boudsocq M, Willmann MR, McCormack M, Lee H, Shan L, He P, Bush J, Cheng S-H, Sheen J. 2010. Differential innate immune signalling via $Ca^{(2+)}$ sensor protein kinases. *Nature* **464**: 418–422.

Brand T, Petersen F, Demann J, Wichura A. 2021. First report on *Pythium myriotylum* as pathogen on duckweed (*Lemna minor* L.) in hydroponic systems in Germany. *Journal für Kulturpflanzen* **73**: 316–323.

van der Burgh AM, Jelle P, Robatzek S, Joosten MHAJ. 2019. Kinase activity of SOBIR1 and BAK1 is required for immune signalling. *Molecular Plant Pathology* **20**: 410–422.

CABI. 2021. Duckweed. In: *Invasive species compendium.* Wallingford, UK: CAB International. [WWW document] URL www.cabi.org/isc [accessed 2 November 2021].

Cai R, Lewis J, Yan S, Liu H, Clarke CR, Campanile F, Almeida NF, Studholme DJ, Lindeberg M, Schneider D *et al.* 2011. The plant pathogen *Pseudomonas syringae* pv *tomato* is genetically monomorphic and under strong selection to evade tomato immunity. *PLoS Pathogens* **7**: e1002130.

Camacho C, Coulouris G, Avagyan V, Ma N, Papadopoulos J, Bealer K, Madden TL. 2009. BLAST+: architecture and applications. *BMC Bioinformatics* **10**: 42–421.

Cao H, Bowling SA, Gordon AS, Dong X. 1994. Characterization of an Arabidopsis mutant that is nonresponsive to inducers of systemic acquired resistance. *Plant Cell* **6**: 1583–1592.

Chanroj S, Jaiprasert A, Issaro N. 2021. A novel technique for recombinant protein expression in duckweed (*Spirodela polyrhiza*) turions. *Journal of Plant Biotechnology* **48**: 156–164.

Chen Y-C, Holmes EC, Rajniak J, Kim J-G, Tang S, Fischer CR, Mudgett MB, Sattely ES. 2018. N-hydroxy-pipecolic acid is a mobile metabolite that induces systemic disease resistance in Arabidopsis. *Proceedings of the National Academy of Sciences, USA* **115**: E4920–E4929.

Clarke J, Liu Y, Klessig DF, Dong X. 1998. Uncoupling PR gene expression from NPR1 and bacterial resistance: characterization of the dominant Arabidopsis *cpr6-1* mutant. *Plant Cell* **10**: 557–569.

Corwin JA, Kliebenstein DJ. 2017. Quantitative resistance: more than just perception of a pathogen. *Plant Cell* **29**: 655–665.

Crawford DJ, Landolt E, Les DH, Kimball RT. 2006. Speciation in Duckweeds (Lemnaceae): phylogenetic and ecological inferences. *Aliso* **22**: 231–242.

Cui H, Gobbato E, Kracher B, Qiu J, Bautor J, Parker JE. 2017. A core function of *EDS1* with *PAD4* Is to protect the salicylic acid defense sector in Arabidopsis immunity. *New Phytologist* **213**: 1802–1817.

Czeczuga B, Godlewska A, Kiziewicz B, Muszyńska E, Mazalska B. 2005. Effect of aquatic plants on the abundance of aquatic zoosporic fungus species. *Polish Journal of Applied Psychology* **14**: 283–297.

Dai Z, Sheridan JM, Gearing LJ, Moore DL, Su S, Wormald S, Wilcox S, O'Connor L, Dickins RA, Blewitt ME *et al.* 2014. EDGER: a versatile tool for the analysis of shRNA-Seq and CRISPR-Cas9 genetic screens. *F1000Research* **3**: 95.

Davis KR, Schott E, Ausubel FM. 1991. Virulence of selected phytopathogenic Pseudomonads in *Arabidopsis thaliana*. *Molecular Plant–Microbe Interactions* **4**: 477–488.

Dong J, Chen C, Chen Z. 2003. Expression profiles of the Arabidopsis *WRKY* gene superfamily during plant defense response. *Plant Molecular Biology* **51**: 21–37.

Emms DM, Kelly S. 2019. ORTHOFINDER: phylogenetic orthology inference for comparative genomics. *Genome Biology* **20**: 238.

Feil H, Feil WS, Chain P, Larimer F, DiBartolo G, Copeland A, Lykidis A, Trong S, Nolan M, Goltsman E *et al.* 2005. Comparison of the complete genome sequences of *Pseudomonas syringae* pv *syringae* B728a and pv *tomato* DC3000. *Proceedings of the National Academy of Sciences, USA* **102**: 11064–11069.

Fisch C. 1884. Beitrage Zur Kenntnis Der Chytridiaceen, Sitzungsber. *Physics in Medicine & Biology* **16**: 29–66.

Flaishman MA, Hadar E, Hallak-Herr E. 1997. First report of *Pythium myriotylum* on *Lemna gibba* in Israel. *Plant Disease* **81**: 550.

Fonseca S, Chini A, Hamberg M, Adie B, Porzel A, Kramell R, Miersch O, Wasternack C, Solano R. 2009. (+)-7-*iso*-Jasmonoyl-L-isoleucine is the endogenous bioactive jasmonate. *Nature Chemical Biology* **5**: 344–350.

Gao M, Wang X, Wang D, Fang X, Ding X, Zhang Z, Bi D, Cheng YT, Chen S, Li X *et al.* 2009. Regulation of cell death and innate immunity by two receptor-like kinases in Arabidopsis. *Cell Host & Microbe* **6**: 34–44.

Gaumann EA. 1928. V. Archimycetes. In: Sinnott EW, ed. *Comparative morphology of fungi*. New York, NY, USA: McGraw-Hill, 17–20.

Girija AM, Kinathi BK, Madhavi MB, Ramesh P, Vungarala S, Patel HK, Sonti RV. 2017. Rice leaf transcriptional profiling suggests a functional interplay between *Xanthomonas Oryzae* pv *oryzae* lipopolysaccharide and extracellular polysaccharide in modulation of defense responses during infection. *Molecular Plant–Microbe Interactions* **30**: 16–27.

Gutiérrez-Barranquero JA, Cazorla FM, de Vicente A. 2019. *Pseudomonas syringae* pv *syringae* associated with mango trees, a particular pathogen within the 'hodgepodge' of the *Pseudomonas syringae* complex. *Frontiers in Plant Science* **10**: 570.

Harkess A, McLoughlin F, Bilkey N, Elliott K, Emenecker R, Mattoon E, Miller K, Czymmek K, Vierstra RD, Meyers BC *et al.* 2021. Improved *Spirodela polyrhiza* genome and proteomic analyses reveal a conserved chromosomal structure with high abundance of chloroplastic proteins favoring energy production. *Journal of Experimental Botany* **72**: 2491–2500.

Hauck P, Thilmony R, He SY. 2003. A *Pseudomonas syringae* type III effector suppresses cell wall-based extracellular defense in susceptible Arabidopsis plants. *Proceedings of the National Academy of Sciences, USA* **100**: 8577–8582.

Ho EKH, Bartkowska M, Wright SI, Agrawal AF. 2019. Population genomics of the facultatively asexual duckweed *Spirodela polyrhiza*. *New Phytologist* **224**: 1361–1371.

Hoang PNT, Michael TP, Gilbert S, Philomena Chu S, Motley T, Appenroth KJ, Schubert I, Lam E. 2018. Generating a high-confidence reference genome map of the greater duckweed by integration of cytogenomic, optical mapping, and Oxford Nanopore Technologies. *The Plant Journal* **96**: 670–684.

Hoang PTN, Fiebig A, Novák P, Macas J, Cao HX, Stepanenko A, Chen G, Borisjuk N, Scholz U, Schubert I. 2020. Chromosome-scale genome assembly for the duckweed *Spirodela intermedia*, integrating cytogenetic maps, PacBio and Oxford Nanopore libraries. *Scientific Reports* **10**: 19230.

Hruz T, Laule O, Szabo G, Wessendorp F, Bleuler S, Oertle L, Widmayer P, Gruissem W, Zimmermann P. 2008. GENEVESTIGATOR v.3: a reference expression database for the meta-analysis of transcriptomes. *Advances in Bioinformatics* **2008**: 420747.

Huang H, Thu TNT, He X, Gravot A, Bernillon S, Ballini E, Morel J-B. 2017. Increase of fungal pathogenicity and role of plant glutamine in nitrogen-induced susceptibility (NIS) to rice blast. *Frontiers in Plant Science* **8**: 265.

Huerta-Cepas J, Forslund K, Coelho LP, Szklarczyk D, Jensen LJ, von Mering C, Bork P. 2017. Fast genome-wide functional annotation through orthology assignment by eggNOG-Mapper. *Molecular Biology and Evolution* **34**: 2115–2122.

Huot B, Castroverde CDM, Velásquez AC, Hubbard E, Pulman JA, Yao J, Childs KL, Tsuda K, Montgomery BL, He SY. 2017. Dual impact of elevated temperature on plant defence and bacterial virulence in Arabidopsis. *Nature Communications* **8**: 1808.

Huot B, Yao J, Montgomery BL, He SY. 2014. Growth-defense tradeoffs in plants: a balancing act to optimize fitness. *Molecular Plant* **7**: 1267–1287.

Institute of Medicine (US) Committee on Resource Sharing, Berns KI, Bond EC, Manning FJ. 1996. *The american type culture collection*. Washington, DC, USA: National Academies Press (US).

Ishiga Y, Ishiga T, Uppalapati SR, Mysore KS. 2011. Arabidopsis seedling flood-inoculation technique: a rapid and reliable assay for studying plant–bacterial interactions. *Plant Methods* **7**: 32.

Ishiga Y, Ishiga T, Uppalapati SR, Mysore KS. 2013. Jasmonate ZIM-Domain (JAZ) protein regulates host and nonhost pathogen-induced cell death in tomato and *Nicotiana Benthamiana*. *PLoS ONE* **8**: e75728.

Jirage D, Tootle TL, Reuber TL, Frost LN, Feys BJ, Parker JE, Ausubel FM, Glazebrook J. 1999. *Arabidopsis thaliana PAD4* encodes a lipase-like gene that is important for salicylic acid signaling. *Proceedings of the National Academy of Sciences, USA* **96**: 13583–13588.

Johanndrees O, Baggs EL, Uhlmann C, Locci F, Läßle HL, Melkonian K, Käufer K, Dongus JA, Nakagami H, Krasileva KV *et al.* 2021. Differential EDS1 requirement for cell death activities of plant TIR-Domain proteins. *bioRxiv*. doi: 10.1101/2021.11.29.470438.

Katagiri F, Thilmony R, He SY. 2002. The *Arabidopsis thaliana–Pseudomonas syringae* interaction. *The Arabidopsis Book* **1**: e0039.

Kazan K, Rusu A, Marcus JP, Goulter KC, Manners JM. 2002. Enhanced quantitative resistance to *Leptosphaeria maculans* conferred by expression of a novel antimicrobial peptide in canola (*Brassica napus* L.). *Molecular Breeding* **10**: 63–70.

Kemmerling B, Halter T, Mazzotta S, Mosher S, Nürnberger T. 2011. A genome-wide survey for Arabidopsis leucine-rich repeat receptor kinases implicated in plant immunity. *Frontiers in Plant Science* **2**: 88.

Kim D, Langmead B, Salzberg SL. 2015. HISAT: a fast spliced aligner with low memory requirements. *Nature Methods* **12**: 357–360.

Ko S-M, Sun H-J, Oh MJ, Song I-J, Kim M-J, Sin H-S, Goh C-H, Kim Y-W, Lim P-O, Lee H-Y *et al.* 2011. Expression of the protective antigen for PEDV in transgenic duckweed, *Lemna minor*. *Horticulture, Environment, and Biotechnology* **52**: 511–515.

Kumar S, Stecher G, Suleski M, Blair Hedges S. 2017. TimeTree: a resource for timelines, timetrees, and divergence times. *Molecular Biology and Evolution* **34**: 1812–1819.

Lamesch P, Berardini TZ, Li D, Swarbreck D, Wilks C, Sasidharan R, Muller R, Dreher K, Alexander DL, Garcia-Hernandez M *et al.* 2012. The Arabidopsis Information Resource (TAIR): improved gene annotation and new tools. *Nucleic Acids Research* **40**: D1202–D1210.

Landolt E. 1992. Lemnaceae duckweed family. *Journal of the Arizona-Nevada Academy of Science* **26**: 10–14.

Lapin D, Kovacova V, Sun X, Dongus JA, Bhandari D, von Born P, Bautor J, Guarneri N, Rzemieniewski J, Stuttmann J *et al.* 2019. A coevolved *EDS1-SAG101-NRG1* module mediates cell death signaling by TIR-domain immune receptors. *Plant Cell* **31**: 2430–2455.

Liebrand TWH, van den Berg GCM, Zhang Z, Smit P, Cordewener JHG, America AHP, Sklenar J, Jones AME, Tameling WIL, Robatzek S *et al.* 2013. Receptor-like kinase SOBIR1/EVR interacts with receptor-like proteins in plant immunity against fungal infection. *Proceedings of the National Academy of Sciences, USA* **110**: 10010–10015.

Liu Y, Wang Y, Shuqing X, Tang X, Zhao J, Changjiang Y, He G, Hua X, Wang S, Tang Y *et al.* 2019. Efficient genetic transformation and CRISPR/Cas9-mediated genome editing in *Lemna Aequinoctialis*. *Plant Biotechnology Journal* **17**: 2143–2152.

Lolle S, Stevens D, Coaker G. 2020. Plant NLR-triggered immunity: from receptor activation to downstream signaling. *Current Opinion in Immunology* **62**: 99–105.

Madeira F, Park YM, Lee J, Buso N, Gur T, Madhusoodanan N, Basutkar P, Tivey ARN, Potter SC, Finn RD *et al.* 2019. The EMBL-EBI search and sequence analysis tools APIs in 2019. *Nucleic Acids Research* **47**: W636–W641.

Marcus JP, Goulter KC, Green JL, Harrison SJ, Manners JM. 1997. Purification, characterisation and cDNA cloning of an antimicrobial peptide from *Macadamia Integrifolia*. *European Journal of Biochemistry* **244**: 743–749.

Martins PMM, Merfa MV, Takita MA, De Souza AA. 2018. Persistence in phytopathogenic bacteria: do we know enough? *Frontiers in Microbiology* **9**: 1099.

Matthysse AG, Stretton S, Dandie C, McClure NC, Goodman AE. 1996. Construction of gfp vectors for use in gram-negative bacteria Other than *Escherichia coli*. *FEMS Microbiology Letters* **145**: 87–94.

McManus AM, Nielsen KJ, Marcus JP, Harrison SJ, Green JL, Manners JM, Craik DJ. 1999. MiAMP1, a novel protein from *Macadamia integrifolia* adopts a greek key β-barrel fold unique amongst plant antimicrobial proteins. *Journal of Molecular Biology* **293**: 629–638.

Michael TP, Bryant D, Gutierrez R, Borisjuk N, Chu P, Zhang H, Xia J, Zhou J, El Baidouri M, ten Hallers B *et al.* 2017. Comprehensive definition of genome features in *Spirodela Polyrhiza* by high-depth physical mapping and short-read DNA sequencing strategies. *The Plant Journal* **89**: 617–635.

Michael TP, Ernst E, Hartwick N, Chu P, Bryant D, Gilbert S, Ortleb S, Baggs EL, Sowjanya Sree K, Appenroth KJ *et al.* 2020. Genome and time-of-day transcriptome of *Wolffia australiana* link morphological minimization with gene loss and less growth control. *Genome Research* **31**: 225–238.

Mittal S, Davis KR. 1995. Role of the phytotoxin coronatine in the infection of *Arabidopsis thaliana* by *Pseudomonas syringae* pv *tomato*. *Molecular Plant–Microbe Interactions* **8**: 165–171.

Moore RA, Starratt AN, Ma S-W, Morris VL, Cuppels DA. 1989. Identification of a chromosomal region required for biosynthesis of the phytotoxin coronatine by *Pseudomonas syringae* pv *tomato*. *Canadian Journal of Microbiology* **35**: 910–917.

Mudgett MB, Staskawicz BJ. 1999. Characterization of the *Pseudomonas syringae* pv *tomato* AvrRpt2 Protein: demonstration of secretion and processing during bacterial pathogenesis. *Molecular Microbiology* **32**: 927–941.

Nandety RS, Caplan JL, Cavanaugh K, Perroud B, Wroblewski T, Michelmore RW, Meyers BC. 2013. The role of TIR-NBS and TIR-X proteins in plant basal defense responses. *Plant Physiology* **162**: 1459–1472.

Nelson DR, Schuler MA, Paquette SM, Werck-Reichhart D, Bak S. 2004. Comparative genomics of rice and Arabidopsis. analysis of 727 *Cytochrome* P450 genes and pseudogenes from a monocot and a dicot. *Plant Physiology* **135**: 756–772.

Ngou BP, Man H-KA, Ding P, Jones JDG. 2021. Mutual potentiation of plant immunity by cell-surface and intracellular receptors. *Nature* **592**: 110–115.

Nishimura T, Mochizuki S, Ishii-Minami N, Fujisawa Y, Kawahara Y, Yoshida Y, Okada K, Ando S, Matsumura H, Terauchi R *et al.* 2016. *Magnaporthe oryzae* glycine-rich secretion protein, Rbf1 critically participates in pathogenicity through the focal formation of the biotrophic interfacial complex. *PLoS Pathogens* **12**: e1005921.

O'Brien AM, Laurich J, Lash E, Frederickson ME. 2020. Mutualistic outcomes across plant populations, microbes, and environments in the duckweed *Lemna minor*. *Microbial Ecology* **80**: 384–397.

Oberacker P, Stepper P, Bond DM, Höhn S, Focken J, Meyer V, Schelle L, Sugrue VJ, Jeunen G-J, Moser T *et al.* 2019. Bio-On-Magnetic-Beads (BOMB): open platform for high-throughput nucleic acid extraction and manipulation. *PLOS Biology* **17**: e3000107.

Offor BC, Dubery IA, Piater LA. 2020. Prospects of gene knockouts in the functional study of MAMP-triggered immunity: a review. *International Journal of Molecular Sciences* **21**: 2540.

Ou S, Su W, Liao Y, Chougule K, Agda JRA, Hellinga AJ, Lugo CSB, Elliott TA, Ware D, Peterson T *et al.* 2019. Benchmarking transposable element annotation methods for creation of a streamlined, comprehensive pipeline. *Genome Biology* **20**: 275.

Ouyang S, Zhu W, Hamilton J, Lin H, Campbell M, Childs K, Thibaud-Nissen F, Malek RL, Lee Y, Zheng L *et al.* 2007. The TIGR rice genome annotation resource: improvements and new features. *Nucleic Acids Research* **35**: D883–D887.

Parte AC, Carbasse JS, Meier-Kolthoff JP, Reimer LC, Göker M. 2020. List of prokaryotic names with standing in nomenclature (LPSN) moves to the DSMZ. *International Journal of Systematic and Evolutionary Microbiology* **70**: 5607–5612.

Peng Z, Ying H, Xie J, Potnis N, Akhunova A, Jones J, Liu Z, White FF, Liu S. 2016. Long read and single molecule DNA sequencing simplifies genome assembly and TAL effector gene analysis of *Xanthomonas translucens*. *BMC Genomics* **17**: 21.

Pertea M, Pertea GM, Antonescu CM, Chang T-C, Mendell JT, Salzberg SL. 2015. StringTie enables improved reconstruction of a transcriptome from RNA-Seq reads. *Nature Biotechnology* **33**: 290–295.

Potnis N, Timilsina S, Strayer A, Shantharaj D, Barak JD, Paret ML, Vallad GE, Jones JB. 2015. Bacterial spot of tomato and pepper: diverse *Xanthomonas* species with a wide variety of virulence factors posing a worldwide challenge. *Molecular Plant Pathology* **16**: 907–920.

Pruitt RN, Locci F, Wanke F, Zhang L, Saile SC, Joe A, Karelina D, Hua C, Fröhlich K, Wan W-L *et al.* 2021. The EDS1–PAD4–ADR1 node mediates Arabidopsis pattern-triggered immunity. *Nature* **598**: 495–499.

Rawat N, Chiruvuri Naga N, Raman Meenakshi S, Nair S, Bentur JS. 2012. A novel mechanism of gall midge resistance in the rice variety kavya revealed by microarray analysis. *Functional & Integrative Genomics* **12**: 249–264.

Rejmankova E, Blackwell M, Culley DD. 1986. *Dynamics of fungal infection in duckweeds (Lemnaceae)*, vol. **87**. Zürich, Switzerland: Veroff Geobot, Institutes Der ETH, Stiftung Rübel, 178–189.

Richard MMS, Gratias A, Meyers BC, Geffroy V. 2018. Molecular mechanisms that limit the costs of NLR-mediated resistance in plants. *Molecular Plant Pathology* **19**: 2516–2523.

Roberts M, Tang S, Stallmann A, Dangl JL, Bonardi V. 2013. Genetic requirements for signaling from an autoactive plant NB-LRR intracellular innate immune receptor. *PLoS Genetics* **9**: e1003465.

Roden JA, Belt B, Ross JB, Tachibana T, Vargas J, Mudgett MB. 2004. A genetic screen to isolate type III effectors translocated into pepper cells during *Xanthomonas* infection. *Proceedings of the National Academy of Sciences, USA* **101**: 16624–16629.

Salguero-Linares J, Serrano I, Ruiz-Solani N, Salas-Gómez M, Phukan UJ, Manuel González V, Bernardo-Faura M, Valls M, Rengel D, Coll NS. 2021. Robust transcriptional indicators of plant immune cell death revealed by spatio-temporal transcriptome analyses. *bioRxiv*. doi: 10.1101/2021.10.06.463031.

Sandler G, Bartkowska M, Agrawal AF, Wright SI. 2020. Estimation of the SNP mutation rate in two vegetatively propagating species of duckweed. *G3 Genes Genomes Genetics* **10**: 4191–4200.

Sarris PF, Cevik V, Dagdas G, Jones JDG, Krasileva KV. 2016. Comparative analysis of plant immune receptor architectures uncovers host proteins likely targeted by pathogens. *BMC Biology* **14**: 8.

Schwartz AR, Morbitzer R, Lahaye T, Staskawicz BJ. 2017. TALE-Induced bHLH transcription factors that activate a pectate lyase contribute to water soaking in bacterial spot of tomato. *Proceedings of the National Academy of Sciences, USA* **114**: E897–E903.

Shao Z-Q, Xue J-Y, Ping W, Zhang Y-M, Yue W, Hang Y-Y, Wang B, Chen J-Q. 2016. Large-scale analyses of angiosperm nucleotide-binding site-leucine-rich repeat genes reveal three anciently diverged classes with distinct evolutionary patterns. *Plant Physiology* **170**: 2095–2109.

Shao Z-Q, Xue J-Y, Wang Q, Wang B, Chen J-Q. 2019. Revisiting the origin of plant NBS-LRR genes. *Trends in Plant Science* **24**: 9–12.

Simão FA, Waterhouse RM, Ioannidis P, Kriventseva EV, Zdobnov EM. 2015. BUSCO: assessing genome assembly and annotation completeness with single-copy orthologs. *Bioinformatics* **31**: 3210–3212.

Sreedharan A, Penaloza-Vazquez A, Kunkel BN, Bender CL. 2006. CorR regulates multiple components of virulence in *Pseudomonas syringae* pv *tomato* DC3000. *Molecular Plant–Microbe Interactions* **19**: 768–779.

Staskawicz B, Dahlbeck D, Keen N, Napoli C. 1987. Molecular characterization of cloned avirulence genes from Race 0 and Race 1 of *Pseudomonas syringae* pv *glycinea*. *Journal of Bacteriology* **169**: 5789–5794.

Stephens C, Kazan K, Goulter KC, Maclean DJ, Manners JM. 2005. The mode of action of the plant antimicrobial peptide MiAMP1 differs from that of its structural homologue, the yeast killer toxin WmKT. *FEMS Microbiology Letters* **243**: 205–210.

Su H, Zhao Y, Jiang J, Lu Q, Li Q, Luo Y, Zhao H, Wang M. 2014. Use of duckweed (*Landoltia punctata*) as a fermentation substrate for the production of higher alcohols as biofuels. *Energy & Fuels* **28**: 3206–3216.

Thilmony R, Underwood W, He SY. 2006. Genome-wide transcriptional analysis of the *Arabidopsis thaliana* interaction with the plant pathogen *Pseudomonas syringae* pv *tomato* DC3000 and the human pathogen *Escherichia coli* O157:H7. *The Plant Journal* **46**: 34–53.

Tian H, Zhongshou W, Chen S, Ao K, Huang W, Yaghmaiean H, Sun T, Xu F, Zhang Y, Wang S *et al.* 2021. Activation of TIR signalling boosts pattern-triggered immunity. *Nature* **598**: 500–503.

Tomato Genome Consortium. 2012. The tomato genome sequence provides insights into fleshy fruit evolution. *Nature* **485**: 635–641.

Umezawa T, Shinozaki K, Mizoguchi M, Takasaki H, Yamaguchi-Shinozaki K, Kidokoro S, Nakashima K, Fujita Y. 2010. Two closely related subclass II SnRK2 protein kinases cooperatively regulate drought-inducible gene expression. *Plant & Cell Physiology* **51**: 842–847.

Van Hoeck A, Horemans N, Monsieurs P, Cao HX, Vandenhove H, Blust R. 2015. The first draft genome of the aquatic model plant *Lemna minor* opens the route for future stress physiology research and biotechnological applications. *Biotechnology for Biofuels* **8**: 188.

Vanky K. 1981. Two new genera of *Ustilaginales*: *Nannfeldtiomyces* and *Pseudodoassansia*, and a survey of allied genera. *Sydowia Annales Mycologici* **34**: 167–178.

Velásquez AC, Oney M, Huot B, Shu X, He SY. 2017. Diverse mechanisms of resistance to *Pseudomonas syringae* in a thousand natural accessions of *Arabidopsis thaliana*. *New Phytologist* **214**: 1673–1687.

Wagner S, Stuttmann J, Rietz S, Guerois R, Brunstein E, Bautor J, Niefind K, Parker JE. 2013. Structural basis for signaling by exclusive *EDS1* heteromeric complexes with *SAG101* or *PAD4* in plant innate immunity. *Cell Host & Microbe* **14**: 619–630.

Wang W, Haberer G, Gundlach H, Gläßer C, Nussbaumer T, Luo MC, Lomsadze A, Borodovsky M, Krerstetter RA, Shanklin J *et al.* 2014. The *Spirodela polyrhiza* genome reveals insights into its neotenous reduction fast growth and aquatic lifestyle. *Nature Communications* **5**: 3311.

Wasternack C, Xie D. 2010. The genuine ligand of a jasmonic acid receptor: improved analysis of jasmonates is now required. *Plant Signaling & Behavior* **5**: 337–340.

Waterhouse AM, Procter JB, Martin DMA, Clamp M, Barton GJ. 2009. JALVIEW version 2 – a multiple sequence alignment editor and analysis workbench. *Bioinformatics* **25**: 1189–1191.

Wheeler TJ, Eddy SR. 2013. NHMMER: DNA homology search with profile HMMs. *Bioinformatics* **29**: 2487–2489.

Xin X-F, Nomura K, Aung K, Velásquez AC, Yao J, Boutrot F, Chang JH, Zipfel C, He SY. 2016. Bacteria establish an aqueous living space in plants crucial for virulence. *Nature* **539**: 524–529.

Xu S, Stapley J, Gablenz S, Boyer J, Appenroth KJ, Sowjanya Sree K, Gershenzon J, Widmer A, Huber M. 2019. Low genetic variation is associated with low mutation rate in the giant duckweed. *Nature Communications* **10**: 1243.

Xu Y-L, Fang Y, Li Q, Yang G-L, Guo L, Chen G-K, Tan L, He K-Z, Jin Y-L, Zhao H. 2018. Turion, an innovative duckweed-based starch production system for economical biofuel manufacture. *Industrial Crops and Products* **124**: 108–114.

Yang G-L, Fang Y, Ya-Liang X, Tan L, Li Q, Liu Y, Lai F, Jin Y-L, An-Ping D, He K-Z *et al.* 2018. Frond transformation system mediated by *Agrobacterium tumefaciens* for *Lemna minor*. *Plant Molecular Biology* **98**: 319–331.

Yang J, Li G, Shiqi H, Bishopp A, Heenatigala PPM, Kumar S, Duan P, Yao L, Hou H. 2018. A protocol for efficient callus induction and stable transformation of *Spirodela polyrhiza* (L.) Schleiden using *Agrobacterium tumefaciens*. *Aquatic Botany* **151**: 80–86.

Yin J, Jiang L, Wang L, Han X, Guo W, Li C, Zhou Y, Denton M, Zhang P. 2021. A high-quality genome of taro (*Colocasia esculenta* (L.) Schott), one of the world's oldest crops. *Molecular Ecology Resources* **21**: 68–77.

Yuan M, Jiang Z, Bi G, Nomura K, Liu M, Wang Y, Cai B, Zhou J-M, He SY, Xin X-F. 2021a. Pattern-recognition receptors are required for NLR-mediated plant immunity. *Nature* **592**: 105–109.

Yuan M, Ngou BPM, Ding P, Xin X-F. 2021b. PTI-ETI crosstalk: an integrative view of plant immunity. *Current Opinion in Plant Biology* **62**: 102030.

Zhao W, Yang P, Kang L, Cui F. 2016. Different pathogenicities of rice stripe virus from the insect vector and from viruliferous plants. *New Phytologist* **210**: 196–207.

Supporting Information

Additional Supporting Information may be found online in the Supporting Information section at the end of the article.

Dataset S1 Powerpoint presentation of pathogen inoculation symptoms.

Dataset S2 Z-stack microscopy.

Dataset S3 Differentially expressed gene tables *Spirodela polyrhiza*.

Dataset S4 Differentially expressed gene tables *Landoltia punctata*.

Dataset S5 Orthogroup assignment and overlap across pathogen treatments and species.

Fig. S1 PlotMDS for all *Spirodela polyrhiza* RNA-Seq samples before outlier removal.

Fig. S2 PlotMDS for *Spirodela polyrhiza* RNA-Seq samples after outlier removal.

Fig. S3 PlotMDS for all *Landoltia punctata* RNA-Seq samples before outlier removal.

Fig. S4 PlotMDS for *Landoltia punctata* RNA-Seq samples after outlier removal.

Fig. S5 Phylogeny of Nucleotide-binding Leucine-rich repeat Receptor proteins in duckweeds.

Fig. S6 Phylogeny of receptor-like kinase proteins in duckweeds.

Fig. S7 Phylogeny of receptor-like protein type proteins in duckweeds.

Fig. S8 Phylogeny of MiAMP1 domain-containing proteins in duckweed species.

Fig. S9 Symptoms of *Spirodela polyrhiza* populations derived from a single mother frond after infection with *Pst* DC3000.

Fig. S10 Microscopy of frond surface 5 d post flood inoculation with *Pseudomonas syringae* pv *tomato* DC3000.

Fig. S11 Microscopy of duckweed frond surface 5 and 7 d post flood inoculation with *Pseudomonas syringae* pv *tomato* DC3000 hrcC.

Fig. S12 Low bacterial load infection of *Landoltia punctata* 1 month post inoculation.

Fig. S13 Role of coronatine in *Pst* DC3000 infection of *Spirodela polyrhiza*.

Fig. S14 Role of coronatine in *Pst* DC3000 infection of *Spirodela polyrhiza*.

Fig. S15 Salicylic acid phytotoxicity to *Spirodela polyrhiza* upon buffer or *Pst* DC3000 treatment.

Fig. S16 Dissecting microscope images of duckweed 12 d post inoculation with salicylic acid.

Fig. S17 Role of salicylic acid in *Pst* DC3000 infection of *Spirodela polyrhiza*.

Fig. S18 Role of salicylic acid in *Pst* DC3000 infection of *Spirodela polyrhiza*.

Fig. S19 Role of salicylic acid in *Pst* DC3000 infection of *Spirodela polyrhiza*.

Fig. S20 Role of salicylic acid in *Pst* DC3000 infection of *Spirodela polyrhiza*.

Fig. S21 Role of salicylic acid in *Pss* B728a infection of *Landoltia punctata*.

Fig. S22 Role of salicylic acid in *Pss* B728a infection of *Landoltia punctata*.

Fig. S23 Bar chart of number of genes differentially expressed upon bacterial treatments.

Fig. S24 Log_2 fold change of selected gene families following bacterial pathogen exposure of duckweeds.

Fig. S25 Log_2 fold change of homologs of *Arabidopsis thaliana* bacterial responsive genes.

Fig. S26 Differential expression upon pathogen treatment of the duckweed homologs of Arabidopsis salicylic acid marker genes.

Fig. S27 Orthogroups with conserved upregulation upon pathogen treatment of duckweed species and the expression of orthologs in *Arabidopsis thaliana*.

Fig. S28 Heatmap displaying log_2 fold change of rice homologs of duckweed conserved upregulated gene upon pathogen infection.

Table S1 Genome assembly statistics for *Landoltia punctata* 5635 genome and proteome BUSCO scores.

Table S2 Table of common name and duckweed gene IDs homologous to *Arabidopsis thaliana* disease marker genes.

Table S3 Copy number of orthologs/homologs of immune associated genes.

Table S4 Table of *Spirodela polyrhiza* homologs to Arabidopsis immunity genes.

Table S5 Syndrome prevalence upon pathogen treatment of Lemnaceae species.

Table S6 Log_2 fold change of JAZ domain-containing *Spirodela polyrhiza* genes.

Table S7 Log_2 fold change of WRKY domain-containing *Spirodela polyrhiza* genes.

Table S8 Log_2 fold change of MiAMP1 domain-containing *Spirodela polyrhiza* genes.

Table S9 Log_2 fold change of NB-ARC domain-containing *Spirodela polyrhiza* genes.

Table S10 Log_2 fold change of JAZ domain-containing *Landoltia punctata* genes.

Table S11 Log_2 fold change of WRKY domain-containing *Landoltia punctata* genes.

Table S12 Log_2 fold change NBARC domain-containing genes *Landoltia punctata*.

Table S13 Log_2 fold change MiAMP1 domain-containing genes *Landoltia punctata*.

Table S14 Orthologs to *Arabidopsis thaliana* marker genes that are significantly upregulated upon *Pst* treatment $log_2FC > 0.75$ FDR < 0.05 in either *Spirodela polyrhiza* or *Landoltia punctata*.

Table S15 Homologs to *Arabidopsis thaliana* marker genes that are significantly upregulated upon *Pst* treatment $\log_2FC > 1$ FDR < 0.05.

Table S16 Table of duckweed genes homologous of *Arabidopsis thaliana* salicylic acid responsive genes.

Table S17 Log_2 fold change of *Spirodela polyrhiza* genes homologous to *Arabidopsis thaliana* salicylic acid responsive genes.

Table S18 Log_2 fold change of *Landoltia punctata* genes homologs to *Arabidopsis thaliana* salicylic acid responsive genes.

Table S19 Orthogroups upregulated in *Landoltia punctata* and *Spirodela polyrhiza* after *Pst* DC3000 treatment.

Table S20 Log_2 fold change of rice genes homologous to pathogen upregulated duckweed genes.

Please note: Wiley Blackwell are not responsible for the content or functionality of any Supporting Information supplied by the authors. Any queries (other than missing material) should be directed to the *New Phytologist* Central Office.